

Palladium(0) Nanoparticles Stabilized by Phosphorus Dendrimers Containing Coordinating 15-Membered Triolefinic Macrocycles in Periphery

Elena Badetti,[†] Anne-Marie Caminade,^{*,‡} Jean-Pierre Majoral,[‡]
 Marcial Moreno-Mañas,^{†,§} and Rosa M. Sebastián^{*,†}

Department of Chemistry, Universitat Autònoma de Barcelona, Cerdanyola, 08193 Barcelona, Spain, and
 Laboratoire de Chimie de Coordination, LCC-CNRS, 205 route de Narbonne,
 31077 Toulouse, Cedex 04, France

Received May 9, 2007. In Final Form: October 3, 2007

A new family of phosphorus dendrimers containing on their surfaces 3, 6, 12, and 96 15-membered azamacrocycles has been synthesized. The coordinating ability of these macrocycles to palladium(0) atoms allowed the preparation of new dendrimers of several generations containing the corresponding metal complexes and several new nanoparticulated materials, where nanoparticles are stabilized mainly by the complexed dendrimers of the zero, first, and fourth generations. No reduction process of palladium(II) salts was needed to prepare nanoparticles of 2.5–7.9 nm diameter. All the new compounds and materials have been characterized by NMR, IR, elemental analysis and/or matrix-assisted laser desorption ionization time-of-flight (MALDI-TOF) spectrometry, high-resolution transmission electron microscopy, and electron diffraction. Also UV–vis spectra were obtained. The Mizoroki–Heck reaction has been catalyzed in a homogeneous and heterogeneous manner by using four different materials; in all cases, the catalyst could be recovered and reused several times.

1. Introduction

Transition metal nanoparticles attract a great deal of attention; their preparation, structure determination, and applications are topics of current interest.^{1,2} Among other interesting properties, their highly specific surfaces render them attractive in catalysis.^{1f,l,o,p} In general, metallic nanoparticles are defined as having a diameter between 1 and 50 nm. They are surrounded by a shell of an adequate protecting agent that prevents agglomeration.^{1b} The protecting agents can be broadly divided into four categories: (i) those that provide electrostatic stabiliza-

tion (cationic and anionic surfactants); (ii) those that provide stabilization by compounds possessing a functional group endowed with high affinity for metals such as thiols, sulfides, amines, and phosphanes;^{1s} (iii) those that simply entrap nanoparticles such as polymers (e.g., poly(vinylpyrrolidone)), cyclodextrins, and dendrimers, although electrostatic stabilization also operates with polymers;³ and (iv) heavily fluorinated compounds that stabilize metal nanoparticles by unknown mechanisms.^{4,5}

Dendrimers are a very special type of hyperbranched polymers, which are synthesized step by step (generation after generation) to ensure a perfect monodispersity.⁶ Most dendrimers are built with nitrogen as the branching points, but some of us have described several series of dendrimers built with phosphorus as the branching points.⁷ Our main method of synthesis affords

* To whom correspondence should be addressed. Telephone: 34-935814288 (R.M.S.); 33-561333125 (A.-M.C.). Fax: 34-935811265 (R.M.S.); 33-561553003 (A.-M.C.). E-mail: rosamaria.sebastian@uab.es (R.M.S.); caminade@lcc-toulouse.fr (A.-M.C.).

[†] Universitat Autònoma de Barcelona.

[‡] LCC-CNRS.

[§] Deceased on 20th February 2006.

(1) (a) Lewis, L. N. *Chem. Rev.* **1993**, *93*, 2693–2730. (b) Bradley, J. S. *The Chemistry of Transition Metal Colloids. In Cluster and Colloids, From Theory to Applications*; Schmid, G., Ed.; VCH: Weinheim, 1994; pp 459–544. (c) *Metal Clusters in Chemistry*; Braunstein, P., Oro, L., Raithby, P. R., Eds.; Wiley-VCH: Weinheim, 1998. (d) *Nanoparticles and Nanostructured Films. Preparation, Characterization and Applications*; Fendler, J. H., Ed.; Wiley-VCH: Weinheim, 1998. (e) Klabunde, K. J.; Mohs, C. *Nanoparticles and Nanostructured Materials. In Chemistry of Advanced Materials. An Overview*; Interrante, L. V., Hampden-Smith, M. J., Eds.; Wiley-VCH: New York, 1998; Chapter 7, pp 271–327. (f) Aiken, J. D., III; Finke, R. G. *J. Mol. Catal. A: Chem.* **1999**, *145*, 1–44. (g) Templeton, A. C.; Wuelfing, W. P.; Murray, R. W. *Acc. Chem. Res.* **2000**, *33*, 27–36. (h) Rao, C. N. R.; Kulkarni, G. U.; Thomas, P. J.; Edwards, P. P. *Chem. Soc. Rev.* **2000**, *29*, 27–35. (i) Horn, D.; Rieger, J. *Angew. Chem., Int. Ed.* **2001**, *40*, 4330–4361. (j) Reetz, M. T.; Winter, M.; Breinbauer, R.; Thurn-Albrecht, T.; Vogel, W. *Chem.—Eur. J.* **2001**, *7*, 1084–1094. (k) Caruso, F. *Adv. Mater.* **2001**, *13*, 11–22. (l) Bönemann, H.; Richards, R. M. *Eur. J. Inorg. Chem.* **2001**, 2455–2480. (m) Rao, C. N. R.; Kulkarni, G. U.; Thomas, P. J.; Edwards, P. P. *Chem.—Eur. J.* **2002**, *8*, 28–35. (n) *Metal Nanoparticles. Synthesis, Characterization, and Applications*; Feldheim, D. L., Foss, C. A., Jr., Eds.; Marcel Dekker, Inc.: New York, 2002. (o) Roucoux, A.; Schulz, J.; Patin, H. *Chem. Rev.* **2002**, *102*, 3757–3778. (p) Moreno-Mañas, M.; Pleixats, R. *Acc. Chem. Res.* **2003**, *36*, 638–643. (q) Philippot, K.; Chaudret, B. *C. R. Chim.* **2003**, *6*, 1019–1034. (r) For a comprehensive review on gold nanoparticles, see: Daniel, M.-C.; Astruc, D. *Chem. Rev.* **2004**, *104*, 293–346. (s) Chaudret, B. *Top. Organomet. Chem.* **2005**, *16*, 233–259.

(2) For a didactic explanation on the structure and properties of nanoparticles, see: Cox, J. *Chem. Br.* **2003**, 21.

(3) Finke, R. G. *Transition-Metal Nanoclusters. In Metal Nanoparticles. Synthesis, Characterization, and Applications*; Feldheim, D. L., Foss, C. A., Jr., Eds.; Marcel Dekker, Inc.: New York, 2002; Chapter 2, pp 17–54.

(4) (a) Moreno-Mañas, M.; Pleixats, R.; Villarroja, S. *Organometallics* **2001**, *20*, 4524–4528. (b) Moreno-Mañas, M.; Pleixats, R.; Villarroja, S. *Chem. Commun.* **2002**, 60–61. (c) Moreno-Mañas, M.; Pleixats, R.; Tristany, M. *J. Fluorine Chem.* **2005**, *126*, 1435–1439. (d) Serra-Muns, A.; Soler, R.; Badetti, E.; de Mendoza, P.; Moreno-Mañas, M.; Pleixats, R.; Sebastián, R. M.; Vallribera, A. *New J. Chem.* **2006**, *30*, 1584–1594.

(5) For a review, see: Moreno-Mañas, M.; Pleixats, R. *Fluorous Nanoparticles. In Handbook of Fluorous Chemistry*; Gladysz, J. A., Curran, D. P., Horváth, I. T., Eds.; Wiley-VCH: Weinheim, 2004; Chapter 12.2, pp 491–507.

(6) For reviews, see: (a) Newkome, G. R.; Moorefield, C. N.; Vögtle, F., Eds.; *Dendrimers and dendrons. Concepts, syntheses, applications*; Wiley-VCH: Weinheim, 2001. (b) Fréchet, J. M. J.; Tomalia, D. A., Eds.; *Dendrimers and other dendritic polymers*; John Wiley and Sons: Chichester, 2001. (c) Shalley, C. A.; Vögtle, F., Eds.; *Dendrimers V: Functional and Hyperbranched Building*; Springer: Berlin/Heidelberg, 2003.

(7) (a) Majoral, J.-P.; Caminade, A.-M. *Chem. Rev.* **1999**, *99*, 845–880. (b) Launay, N.; Caminade, A.-M.; Lahana, R.; Majoral, J.-P. *Angew. Chem., Int. Ed. Engl.* **1994**, *33*, 1589–1592. (c) Maraval, V.; Caminade, A.-M.; Majoral, J.-P.; Blais, J. C. *Angew. Chem., Int. Ed.* **2003**, *42*, 1822–1826. (d) Caminade, A.-M.; Maraval, V.; Laurent, R.; Majoral, J.-P. *Curr. Org. Chem.* **2002**, *6*, 739–774. (e) Griffe, L.; Poupot, M.; Marchand, P.; Maraval, A.; Turrin, T. O.; Rolland, O.; Métivier, P.; Bacquet, G.; Fournié, J. J.; Caminade, A.-M.; Poupot, R.; Majoral, J.-P. *Angew. Chem., Int. Ed.* **2007**, *46*, 2523–2526. (f) Caminade, A.-M.; Majoral, J.-P. *Acc. Chem. Res.* **2004**, *37*, 341–348. (g) Caminade, A.-M.; Turrin, C. O.; Laurent, R.; Maraval, A.; Majoral, J.-P. *Curr. Org. Chem.* **2006**, *10*, 2333–2355.

—OC₆H₄CH=NNMeP(S) branches and Cl or —OC₆H₄CHO end groups.^{7b} The reactivity of these end groups has already led to various applications of these phosphorus-containing dendrimers in catalysis,^{7d} biology,^{7e} and materials science.^{7f}

The stabilization of nanoparticles by entrapment in the cavity of dendrimers has some precedents.^{8,9} The group of Crooks has investigated the formation of noble metal nanoparticles in the interior of poly(amidoamine) (PAMAM) and poly(propyleneimine) (PPI) dendrimers.⁸ This entrapment strategy consists of introducing a salt of metal in the interior of the dendrimer where coordination with the amino groups fixes up the cations. A reduction step converts the cations into metallic atoms in the interior, which form nanoparticles entrapped by the tridimensional skeleton of the dendrimer. For metals whose cations do not coordinate well with amines, an alternative solution was established. Thus, copper nanoparticles were formed as described, and then a solution of a more noble metal (e.g., Ag⁺) was introduced. Silver cations were reduced by Cu(0) to silver atoms that remain entrapped in the dendrimer in the nanoparticulated form. These precedent works are clear examples of what is known as dendrimer encapsulated nanoparticles (DENs). When nanoparticles are not included in dendrimer structures, we talk about dendrimer-stabilized metal nanoparticles (DSNs). Excellent examples of this last group have been reported. The group of Esumi has prepared silver, platinum, and palladium nanoparticles stabilized by PAMAM and PPI in aqueous and nonaqueous solutions; the effect of the concentration of reactants on the size of the nanoparticles has been studied.⁹ Other examples can also be found in the literature.¹⁰

On the other hand, some of us have been interested in nanoparticles stabilized by heavily fluorinated compounds.^{4,5} During these studies, we came to the intuition that the formation of nanoparticles is favored if the stabilizing molecule features a functional group that coordinates one metal atom. Thus, our attention was attracted to triolefinic 15-membered macrocycles **1** (Figure 1), whose preparation and properties have been described by some of us.¹¹ These macrocycles are excellent coordinating agents for Pd(0) and Pt(0) forming stable complexes **2**. Therefore, they fulfill the conditions to stabilize nanoparticles if appropriate substituents are placed in the aromatic rings, such as polyfluorinated or polyoxyethylenated chains.^{4d} The initial coordination of a palladium atom is guaranteed, and the synthetic procedure for this family of macrocycles is very versatile since the building blocks are arenesulfonamides and 1,4-dihalogeno-2-butene. Many arenesulfonamides or the corresponding sulfonyl chlorides are commercially available.

2. Results and Discussion

Therefore, we endeavored to prepare dendrimeric structures containing 15-membered triolefinic macrocycles to take advantage of the known properties of both structures to synthesize

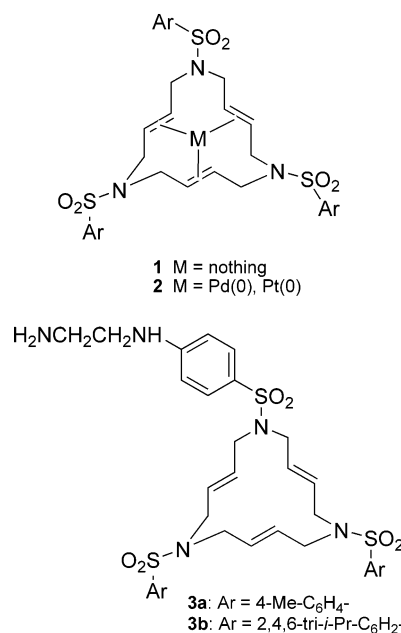


Figure 1. Structures of 15-membered macrocycles (**1** and **3a,b**) and their metal complexes (**2**).

nanoparticles. We have chosen macrocycles **3a**¹² and **3b**¹³ (Figure 1) and phosphorus-containing dendrimers for further elaboration.^{7b} Compounds free of palladium as well as well-defined complexes were characterized by standard methods of molecular chemistry, whereas nanoparticles were determined by high-resolution transmission electron microscopy (HR-TEM), elemental analysis, and infrared spectroscopy. Also, UV-vis experiments confirmed the formation of Pd(0) nanoparticles (Pd NPs). In all cases, electron diffraction of the samples of nanoparticles showed the characteristic pattern of face-centered cubic (fcc) palladium(0) with the average *d*-spacing values given in the Supporting Information. Representative experimental values are indicated in Figure 2 of the text. Theoretical *d*-spacing values corresponding to Pd(0) fcc are as follows: 1.17, 1.38, 1.95, and 2.25 Å.

The combination of the catalytic activity of Pd(0) complexes and nanoparticles and the modular solubility of phosphorus dendrimers in organic solvents has allowed us to obtain interesting easily recoverable and reusable catalysts for organic reactions.

Periphery Modification of Dendrimers. Phosphorus dendrimers containing 3, 6, 12, and 96 aldehyde groups on their surfaces (**4-G₀**,¹⁴ **4-G₁**,¹⁵ **4-G₂**,¹⁶ and **4-G₃**,¹⁶ respectively) have been condensed with macrocycles **3a** and **3b** to obtain the corresponding imines whose C=N bonds were reduced with borohydride derivatives to afford compounds **5** (Schemes 1 and 2).

Dendrimers functionalized with macrocycle **3a** presented limited solubility in ordinary solvents; therefore, we restricted our studies with it to the smaller generations.

In all cases, the completion of the condensation between the dendrimers and macrocycles is shown by ¹H NMR, by the disappearance of the signal corresponding to the aldehyde, together with the appearance of a broad singlet at 8.2–8.3 ppm

(8) For reviews, see: (a) Scott, R. W. J.; Wilson, O. M.; Crooks, R. M. *J. Phys. Chem. B* **2005**, *109*, 692–704. (b) Niu, Y.; Crooks, R. M. *C. R. Chim.* **2003**, *6*, 1049–1059. (c) Crooks, R. M.; Lemon, B. L., III; Sun, L.; Yeung, L. K.; Zhao, M. *Top. Curr. Chem.* **2001**, *212*, 81–135. (d) Crooks, R. M.; Zhao, M.; Sun, L.; Chechik, V.; Yeung, L. K. *Acc. Chem. Res.* **2001**, *34*, 181–190.

(9) (a) Esumi, K. *Top. Curr. Chem.* **2003**, *227*, 31–52. (b) Esumi, K.; Suzuki, A.; Llamaria, A.; Torigoe, K. *Langmuir* **2000**, *16*, 2604–2608. (c) Esumi, K.; Isono, R.; Yoshimura, T. *Langmuir* **2004**, *20*, 237–243.

(10) (a) Garcia, M. E.; Baker, L. A.; Crooks, R. M. *Anal. Chem.* **1999**, *71*, 256–258. (b) Pittelkow, M.; Moth-Poulsen, K.; Boas, U.; Christensen, J. B. *Langmuir* **2003**, *19*, 7682–7684. (c) Knecht, M. R.; Wright, D. W. *Chem. Mater.* **2004**, *16*, 4890–4895.

(11) For reviews, see: (a) Moreno-Mañas, M.; Pleixats, R.; Roglans, A.; Sebastián, R. M.; Vallribera, A. *ARKIVOC* **2004**, (iv), 109–129; available from <http://www.arkat-usa.org>. (b) Moreno-Mañas, M.; Pleixats, R.; Sebastián, R. M.; Vallribera, A.; Roglans, A. *J. Organomet. Chem.* **2004**, *689*, 3669–3684.

(12) Masllorrens, J.; Roglans, A.; Moreno-Mañas, M.; Parella, T. *Organometallics* **2004**, *23*, 2533–2540.

(13) Blanco, B.; Mehdi, A.; Moreno-Mañas, M.; Pleixats, R.; Reyé, C. *Tetrahedron Lett.* **2004**, *45*, 8789–8791.

(14) Launay, N.; Caminade, A.-M.; Lahana, R.; Majoral, J.-P. *Angew. Chem., Int. Ed. Engl.* **1994**, *33*, 1589.

(15) Allcock, H. R.; Austin, P. E. *Macromolecules* **1981**, *14*, 1616–1622.

(16) (a) Slany, M.; Bardají, M.; Casanove, M. J.; Caminade, A.-M.; Majoral, J.-P.; Chaudret, B. *J. Am. Chem. Soc.* **1995**, *117*, 9764–9765. (b) Launay, N.; Caminade, A.-M.; Majoral, J.-P. *J. Organomet. Chem.* **1997**, *529*, 51–58.

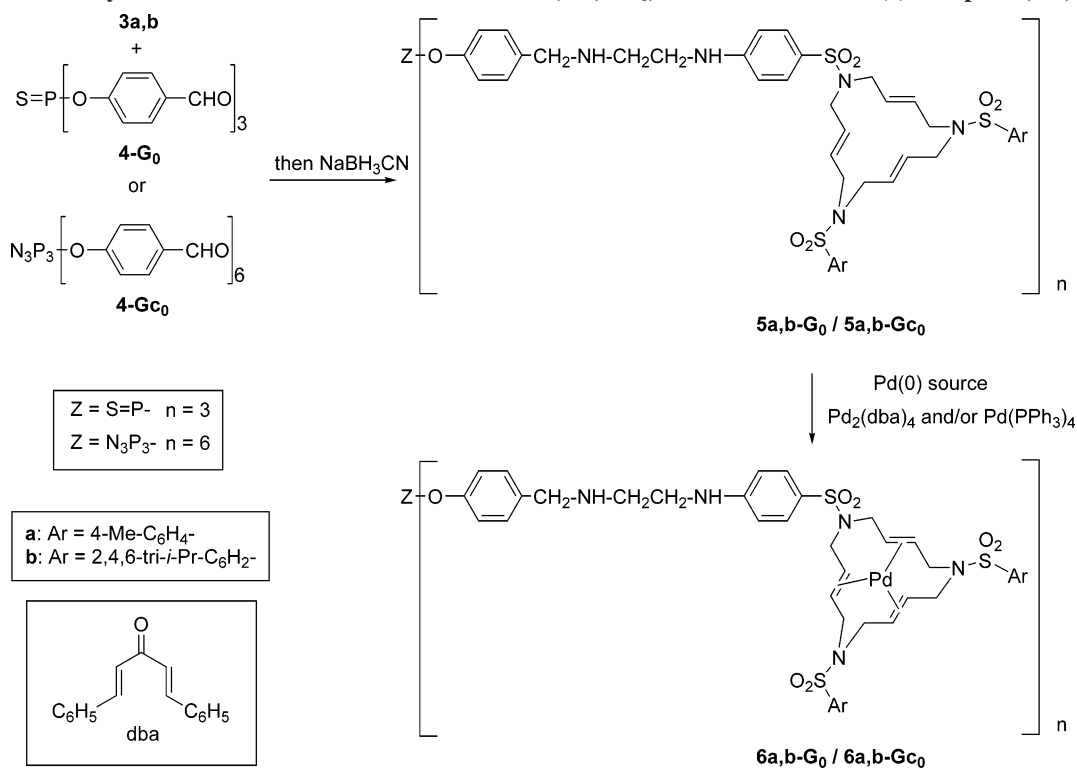
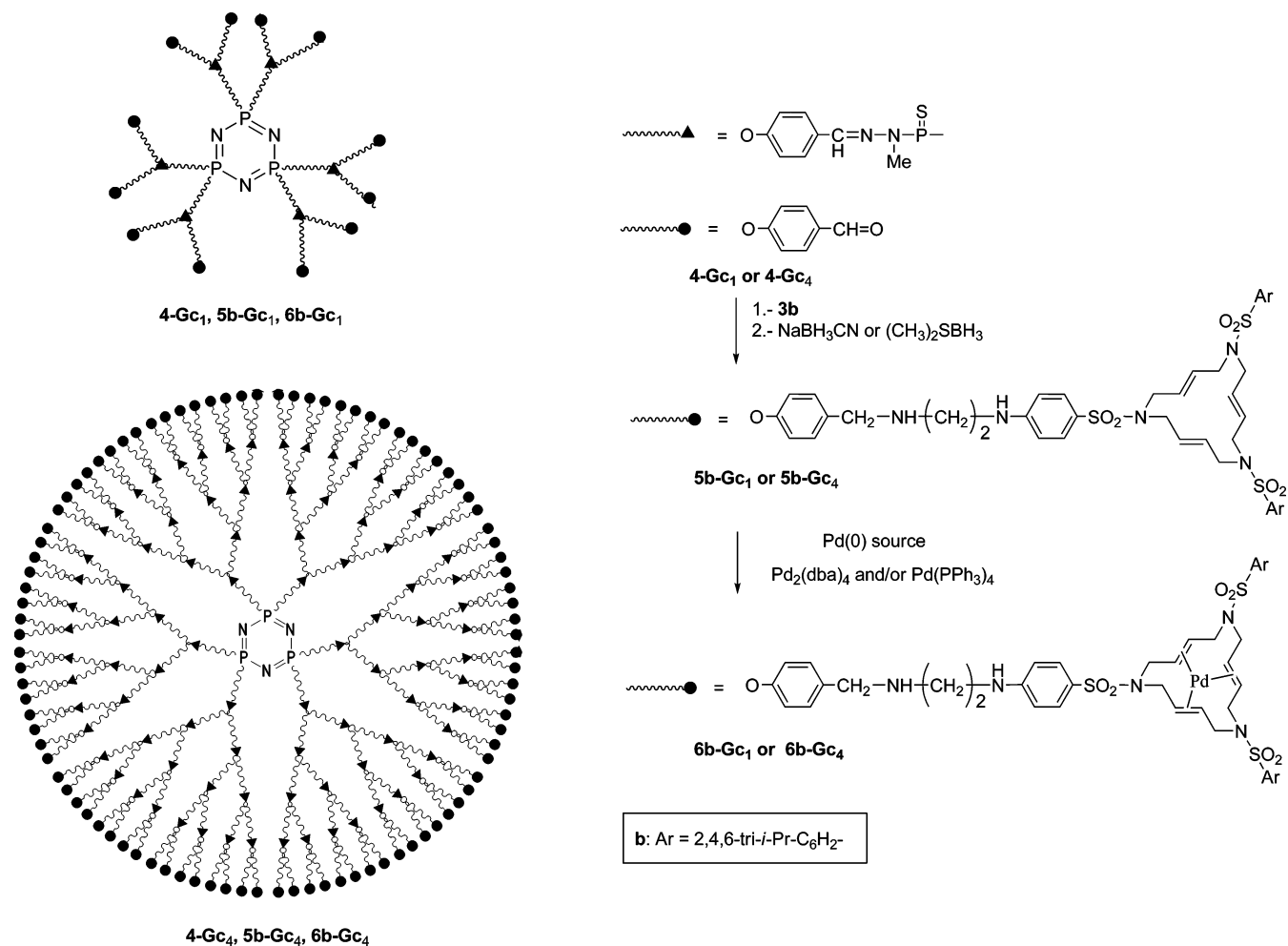
Scheme 1. Synthesis of Dendrimers of Zero Generation, 5a,b-G₀, and Their Palladium(0) Complexes, 6a,b-G₀**Scheme 2. Synthesis of Dendrimers of First and Fourth Generations, 5b-Gc₁ and 5b-Gc₄, and Their Palladium(0) Complexes, 6b-Gc₁ and 6b-Gc₄**

Table 1. Palladium Nanoparticles Stabilized by Dendrimeric Compounds^a

entry	dendrimer	Pd(0) source	initial molar ratio Pd(0)/macrocycle	time	result	Pd % ^b	composition	Ø (nm)	atoms Pd(0)/particle ^c	morphology of nanoparticles ^d	solubility of product in THF
1	5a-G₀	Pd ₂ (dba) ₄	1.17	14 h	nanopart	10.97	Pd₂(6a-G₀)₁ and/or Pd₅(5a-G₀)₁^e	4.2 ± 0.7	2.6 × 10 ³	agglomerated (Figure 2a,b)	no
2	5a-G₀	Pd ₂ (dba) ₄	2.07	14 h	nanopart	11.37	Pd₂(6a-G₀)₁ and/or Pd₅(5a-G₀)₁^e	4.1 ± 0.7	2.4 × 10 ³	well-defined (Figure 2c,d)	no
3	5b-G₀	Pd ₂ (dba) ₄	1.17	14 h	complex	8.20	6b-G₀				yes
4	5b-G₀	Pd ₂ (dba) ₄	3.33	14 h	nanopart	19.35	Pd₇(6b-G₀)₁	4.3 ± 0.7	2.8 × 10 ³	well-defined (Figure 3a,b)	yes
5	5b-G₀	Pd ₂ (dba) ₄	3.33	48 h	nanopart	29.32	Pd₇(6b-G₀)₁	3.4 ± 0.6	1.4 × 10 ³	well-defined in vesicles (Figure 3c)	yes
6	5b-G₀	Pd(PPh ₃) ₄	3.33	14 h	complex		6b-G₀				yes
7	5b-G₀	Pd(PPh ₃) ₄	3.33	6 days	nanopart	22.00	Pd₁₂₋₁₃(5b-G₀)₁	2.5 ± 0.4	5.5 × 10 ²	well-defined (Figure 3d)	yes
8	5a-Gc₀	Pd ₂ (dba) ₄	3.00	7 days	nanopart	15.83	Pd_{7,8}(6a-Gc₀)₁ and/or Pd_{13,8}(5a-Gc₀)₁^e	3.9 ± 1.0	2.1 × 10 ³	agglomerated	no
9	5b-Gc₀	Pd ₂ (dba) ₄	3.00	6 days	nanopart	16.17	Pd₁₁(6b-Gc₀)₁	5.7 ± 0.6	6.5 × 10 ³	agglomerated (Figure 4a)	yes
10	5b-Gc₀	Pd(PPh ₃) ₄	1.33	2 days	complex ^f	12.40	6b-Gc₀				yes
11	5b-Gc₀	Pd(PPh ₃) ₄	3.67	2 days	complex		6b-Gc₀				yes
12	5b-Gc₀	Pd(PPh ₃) ₄	5.00	7 days	nanopart	25.39	Pd₂₃(6b-Gc₀)₁	2.9 ± 0.5	8.6 × 10 ²	well-defined in vesicles (Figure 4b–d)	yes
13	5b-Gc₁	Pd ₂ (dba) ₄	3.08	14 h	nanopart	10.66	Pd₅(6b-Gc₁)₁	3.4 ± 0.4	1.4 × 10 ³	well-defined (Figure 5a)	yes
14	5b-Gc₁	Pd(PPh ₃) ₄	1.83	7 days	nanopart	14.80	Pd₂₂(6b-Gc₁)₁	7.9 ± 2.2	1.7 × 10 ⁴	agglomerated (Figure 5b)	yes
15	5b-Gc₄	Pd ₂ (dba) ₄	1.21	14 h	complex ^g		6b-Gc₄				yes
16	6b-Gc₄	Pd ₂ (dba) ₄	3.00	14 h	nanopart	15.90	Pd₂₃₈(6b-Gc₄)₁	3.2 ± 0.5	1.1 × 10 ³	well-defined (Figure 5c,d)	yes

^a All reactions were performed in THF at 60–70 °C. ^b Determined by elemental analysis. ^c Determined as ($V_{\text{nano}}/V_{\text{atom}}$)^{0.74}; this correction factor is the percentage of space occupation in fcc structures. ^d For more details, see the Supporting Information. ^e NMR spectra could not be registered for solubility reasons; therefore, whether **6a-G₀** and/or **5a-G₀** (entries 1 and 2) or **6a-Gc₀** and/or **5a-Gc₀** (entry 8) is/are present in the protecting shield cannot be ascertained. ^f Elemental analysis showed that the complex was contaminated by black palladium. ^g A small number of Pd(0) nanoparticles of 5.8 nm were observed.

due to the imine proton. Both *E* and *Z* isomers of the imines are presumably formed, as indicated by the appearance of several singlets in the ³¹P NMR spectra for the phosphorus atoms bearing the macrocycles. Reduction of these imines induces the disappearance of the signal at 8.2–8.3 ppm in ¹H NMR and the recovery of a sharp singlet in ³¹P NMR for the phosphorus atoms linked to the macrocycles.

Reaction of Dendrimers with Sources of Palladium(0): Complexes and Nanoparticles. Macrocycles **1** regularly form stable complexes **2** when exposed to palladium(0) (either tetrakis(dibenzylideneacetone)dipalladium(0) (Pd₂(dba)₄) or tetrakis(triphenylphosphino)palladium(0) (Pd(PPh₃)₄)) through the three endocyclic olefins.¹¹ Since macrocycles **1** are better ligands than dba, the transfer of metal from Pd₂(dba)₄ to **1** occurs spontaneously. The transfer of palladium from Pd(PPh₃)₄ to **1** is facilitated by the irreversible oxidation of the phosphine to its oxide. The presence or the absence of palladium(0) coordinated to the macrocycle can be deduced from the NMR spectra. Indeed, free macrocycles present signals for the olefinic protons and carbons at δ ~5.50–5.80 and ~124 ppm, respectively, whereas for palladium complexes strong upfield shifts are observed up to δ 2.50–4.40 (depending on the proton considered) and 78–83 ppm, respectively.¹⁷

Discrete palladium complexes or nanoparticles are expected in the following study, by treatment of all dendrimers prepared

with Pd(0) sources. The entrapping dendrimers could be made of free macrocycles or of complexed macrocycles in the periphery. Both situations should be distinguishable by NMR. All the experiments are shown in Table 1.

When dendrimers containing tolyl groups on the surface were treated with Pd₂(dba)₄, insoluble materials were obtained containing Pd NPs (Table 1, entries 1, 2, and 8). IR spectra showed the presence of a dendritic structure in the material; however, the lack of solubility prevented NMR characterization, and for this reason the definition of the periphery of the dendrimer was not possible. Elemental analysis showed the relation between Pd(0) and the phosphorus atoms. Therefore, the molar formulation of the nanoparticles could be **Pd₅(5a-G₀)₁** or **Pd₂(6a-G₀)₁** (entries 1 and 2) and **Pd_{13,8}(5a-Gc₀)₁** or **Pd_{7,8}(6a-Gc₀)₁** (entry 8) (or mixtures). The use of a different ratio of Pd(0) atoms/macrocycle with **5a-G₀** had no influence on the final size and composition of the nanoparticles. However, working with a higher ratio allowed us to obtain Pd NPs of better quality; agglomeration was not observed (compare entries 1 and 2, and HR-TEM pictures of Figure 2a and c).

All studies conducted with dendrimers containing 2,4,6-triisopropylphenyl groups on the periphery gave products soluble in common organic solvents, that could be studied by NMR experiments, with their compositions being well defined. Some of these dendrimers treated with practically stoichiometric amounts of Pd₂(dba)₄ gave discrete complexes (**6b-G₀** and **6b-Gc₄**, entries 3 and 15, respectively). However, when an excess of this Pd(0) source was used (~3 mol Pd(0) atoms/macrocycle), nanoparticulated materials were isolated (entries 4, 5, 9, 13, and

(17) (a) Cerezo, S.; Cortès, C.; Lago, E.; Molins, E.; Moreno-Mañas, M.; Parella, T.; Pleixats, R.; Torrejón, J.; Vallribera, A. *Eur. J. Inorg. Chem.* **2001**, 1999–2006. (b) Pla-Quintana, A.; Roglans, A.; Vicente, de Julián-Ortiz, J.; Moreno-Mañas, M.; Parella, T.; Benet-Buchholz, J.; Solans, X. *Chem. Eur. J.* **2005**, *11*, 2689–2697.

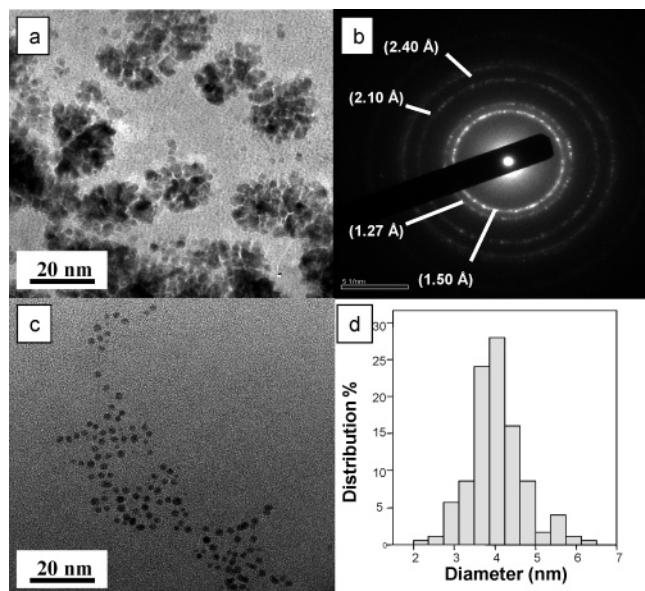


Figure 2. Characterization of nanoparticles of entries 1 and 2 obtained from **5a-G₀** (Table 1). (a) HR-TEM picture of nanoparticles of entry 1. (b) Electron diffraction patterns corresponding to Pd(0) fcc of nanoparticles of entry 1 (Å). (c) HR-TEM picture of nanoparticles of entry 2. (d) Core size distribution histograms of nanoparticles of entry 2.

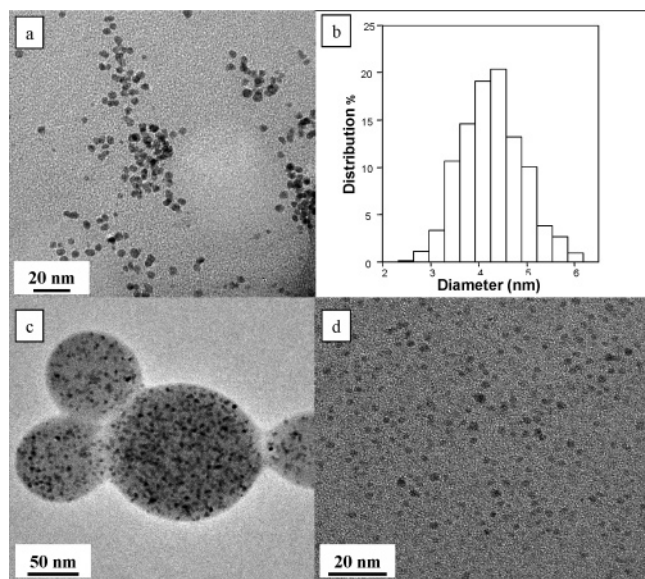


Figure 3. (a and b) HR-TEM picture and core size distribution histogram of nanoparticles of entry 4. (c and d) HR-TEM pictures of nanoparticles of entries 5 (c) and 7 (d). In all cases, materials were obtained from **5b-G₀**.

16). NPs were stabilized by corresponding complexes **6b**, as it was probed by ¹H NMR spectra. Their composition was also determined by elemental analysis. Using **5b-G₀** as the stabilizer, an increase in the percentage of Pd(0) and in the yield of the material was observed when the reaction was performed for longer reaction times; however, no change in the composition of the materials was noticed (compare entries 4 and 5 and see the Experimental section). A different dispersion of nanoparticles was observed between both experiments. The nanoparticles of entry 4 were dispersed; however, the nanoparticles of entry 5 were included in vesicles (Figure 3a and c). This arrangement could be related to the preparation of the samples for HR-TEM. The same effect has also been observed in other materials (*vide infra*).

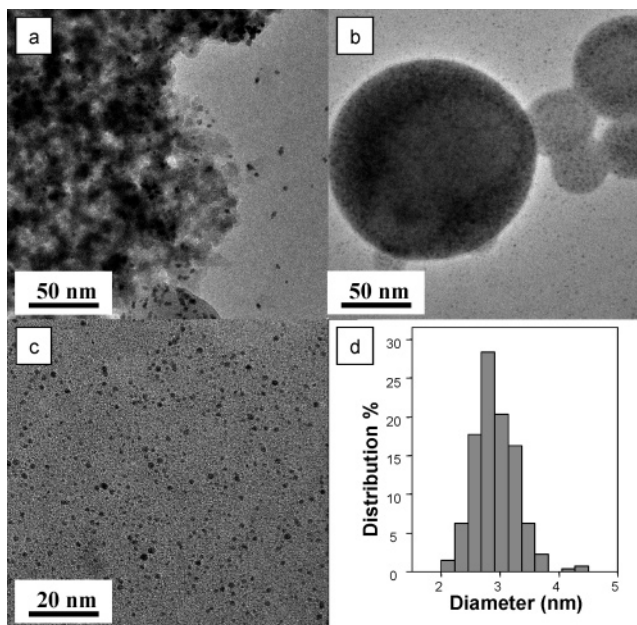


Figure 4. HR-TEM pictures of nanoparticles of entries 9 (a) and 12 (b and c). (d) Core size distribution histogram of nanoparticles of entry 12. Both materials were obtained from **5b-Gc₀**.

UV-vis spectra of **5b-G₀**, **6b-G₀** (entry 3) and **Pd₇(6b-G₀)₁** (entry 5) were obtained (see the Supporting Information). A clear interaction between the Pd(0) atoms and the endocyclic olefins of macrocycles anchored on the surface of the dendrimer was observed in the complex and also in the nanoparticulated material spectra. In the spectrum of this last material, a clear monotonic increase in the absorption was observed which can be matched to the spectrum of Pd NPs in previous literature.¹⁸

When the small dendrimers **5b-G₀** and **5b-Gc₀** were treated with Pd(PPh₃)₄, different products were obtained depending on the reaction time: discrete complexes **6b-G₀** and **6b-Gc₀** were isolated for short reaction times, but nanoparticulated materials were achieved when the reaction was carried out for more than 6 days (compare entries 6 and 7 (Figure 3d) and entries 10/11 and 12 (Figure 4b and c, vesicle organized NPs)). Increasing the initial molar ratio of Pd(0) used for the macrocycle seemed to have no effect on the type of product obtained (compare entries 10 and 11); the reaction time seemed to be the more important variable. Triphenylphosphine oxide was also present in all of the products; its elimination was not possible. It should be mentioned that when the reaction was carried out with dendrimer **5b-G₀**, Pd NPs were stabilized by the free dendrimer and not by the corresponding Pd(0) complex as usual (entry 7); ¹H NMR spectra of the soluble nanoparticulated material confirmed the composition. Decomplexation of the macrocycles has already been observed by the action of temperature.^{4d} These experiments suggested that, in the process of forming nanoparticles, standard organometallic complexation is the first event of the sequence, followed by nanoparticle formation and eventual decomplexation of the macrocycle.^{4d}

For these small dendrimers, the use of Pd(PPh₃)₄ instead of Pd₂(dba)₄ allowed us to obtain Pd NPs of smaller sizes (for **5b-G₀**: 2.5 nm, entry 7, and 3.4 nm, entry 5; for **5b-Gc₀**: 2.9 nm, entry 12, and 5.7 nm, entry 9 (Figure 4)). However, when

(18) (a) Henglein, A. *J. Phys. Chem. B* **2000**, *104*, 6683–6685. (b) Garcia-Martínez, J. C.; Scout, R. W. J.; Crooks, R. M. *J. Am. Chem. Soc.* **2003**, *125*, 11190–11191. (c) Tan, H.; Zhan, T.; Fan, W. Y. *Chem. Phys. Lett.* **2006**, *428*, 352–355. (d) Rao, C. R. K.; Lakshminarayana, V.; Trivedi, D. C. *Mater. Lett.* **2006**, *60*, 3165–3169. (e) Kim, J.-H.; Chung, H.-W.; Lee, T. R. *Chem. Mater.* **2006**, *18*, 4115–4120.

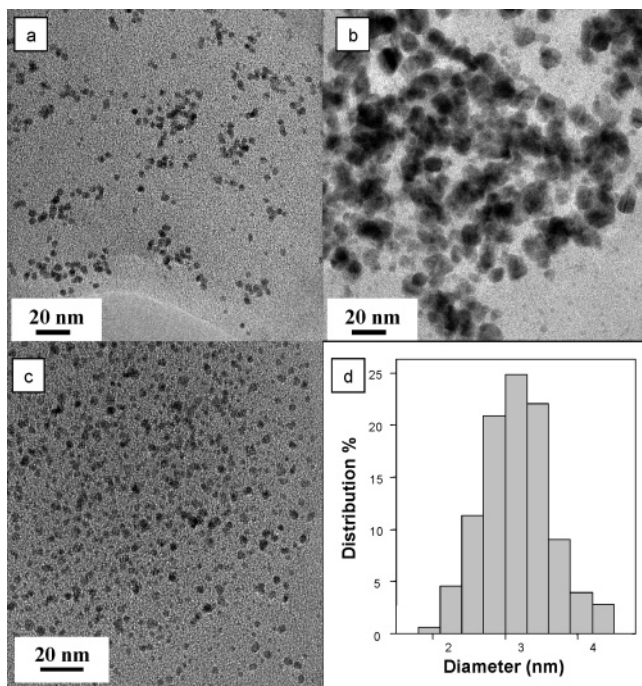


Figure 5. HR-TEM of nanoparticles of entries 13 (a) and 14 (b) obtained from **5b-Gc₁**. HR-TEM picture (c) and core size distribution histogram (d) of nanoparticles of entry 16 obtained from **6b-Gc₄**.

bigger dendrimers were used (**5b-Gc₁** and **5b-Gc₄**) reactions with Pd(PPh₃)₄ gave the worst results. NPs obtained from **5b-Gc₁** were bigger and more agglomerated than those obtained using Pd₂(dba)₄ (7.9 and 3.4 nm, entries 13 and 14, Figure 5a and b respectively). When **5b-Gc₄** was treated with an excess of Pd(PPh₃)₄, neither complete complexation of macrocycles nor nanoparticle formation was achieved after 7 days. The same reaction performed with Pd₂(dba)₄ gave good quality Pd NPs of 3.2 nm (entry 16, Figure 5c and d).

With these results, we can conclude that nanoparticle size did not seem to have any relation to the dendrimer used as the stabilizer. However, the selection of palladium(0) sources in combination with stabilizers is important to determine the size of the nanoparticles, but no rule could be generalized. Pd NPs obtained from Pd₂(dba)₄ required, in general, shorter reaction times.

Compounds or materials containing large amounts of palladium(0) presented broad signals in the ¹H NMR spectra. No phosphorus signals (or very broad ones) could be detected in the ³¹P NMR spectra of soluble materials containing nanoparticles. This effect could be explained by the proximity of the nanoparticles to these atoms which reduces isotropy (reduces mobility); similar effects have been described previously in the literature.¹⁹

At present, we cannot give a definitive answer to how these nanoparticles are stabilized. However, the preparation of soluble nanoparticles includes filtration through Celite without noticeable destruction. IR, UV-vis, and ¹H NMR spectra showed the presence of dendrimers in the materials. So, in conclusion, all these facts confirm that nanoparticles are stabilized by dendrimers. From the composition of the materials and the number of atoms contained in the nanoparticles, it is possible to establish the number

(19) (a) Badia, A.; Gao, W.; Singh, S.; Demers, L.; Cuccia, L.; Reven, L. *Langmuir* **1996**, *12*, 1262–1269. (b) Zelakiewicz, B. S.; De Dios, A. C.; Tong, Y. Y. *J. Am. Chem. Soc.* **2003**, *125*, 18–19. (c) Gopidas, K. R.; Whitesell, J. K.; Fox, M. A. *J. Am. Chem. Soc.* **2003**, *125*, 14168–14180. (d) Kim, K.-S.; Demberelymba, D.; Lee, H. *Langmuir* **2004**, *20*, 556–560. (e) Horinouchi, S.; Yamanoi, Y.; Yonezawa, T.; Mouri, T.; Nishihara, H. *Langmuir* **2006**, *22*, 1880–1884.

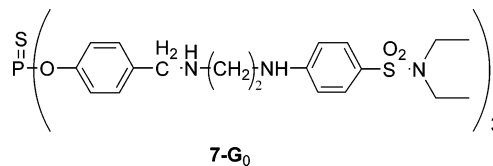


Figure 6. Dendrimer containing the same functional groups as dendrimers previously reported in this article (**5-G₀**) but without macrocycles on its surface.

of dendrimers that could stabilize each nanoparticle. For small dendrimers (zero and first generation), each nanoparticle seemed to be stabilized by multiple dendrimers (37–773, depending on the material; DSNs type). However, for the biggest one (the fourth generation dendrimer), we obtained a smaller ratio (5 dendrimers/nanoparticle).²⁰ In this case, the possibility to have encapsulated nanoparticles should be also considered.

A model dendrimer similar to **5-G₀** has also been prepared (**7-G₀**, Figure 6). This compound does not contain macrocycles on its structure; however, when it was treated with Pd₂(dba)₄, non-homogeneous, agglomerated, badly defined insoluble nanoparticles of 3.8 nm were obtained (see the Supporting Information). The presence of the macrocycles on the surfaces of dendrimers is important to obtain well-defined nanoparticles. Moreover, the solubility of these new materials can also be modulated by the groups contained on the surfaces of the macrocycles. An important role of macrocycles in the stabilization of Pd NPs was also observed in the catalytic tests performed.

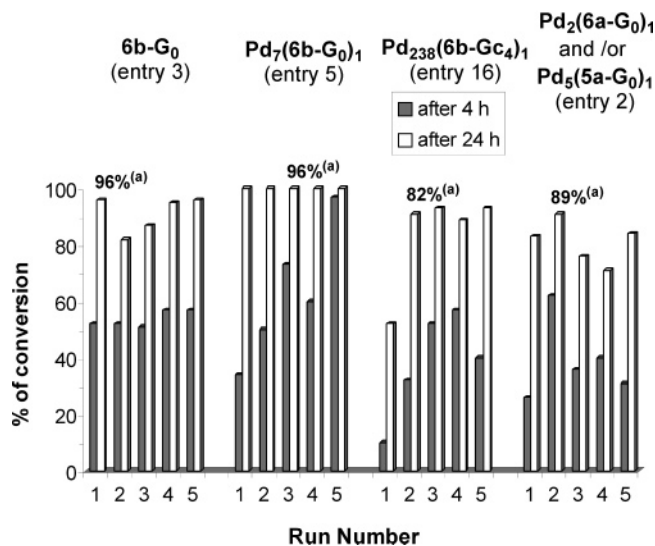
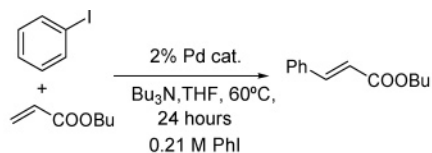
Catalytic Tests. Metal nanoparticles in general, and in particular palladium nanoparticles, have found application in catalysis due to their highly specific surfaces.^{1f,i,o,p,9c} We have described fluoros biphasic systems that permitted recovery and reutilization of palladium nanoparticles as catalysts in Suzuki cross-coupling and in Mizoroki–Heck reactions.^{4a} Phosphorus-containing dendrimers have been previously functionalized by conventional metal ligands on the surface (P, P,N, or N,N ligands), and their complexes have been used as homogeneous catalysts in Michael additions, Knoevenagel and Stille reactions, and arylation reactions; these dendritic catalysts were easily recovered and reused.²¹ Palladium(0)–triolefinic 15-membered macrocycles of type **2** have also been used as catalysts or precatalysts of several organic reactions in homogeneous and heterogeneous manners.^{11,13,22} Nanoparticles stabilized by our 15-membered macrocycles containing long polyfluorinated and polyoxyethylenated chains were good homogeneous catalysts for Heck reactions.^{4d} Several examples of coupling reactions have been catalyzed by entrapped nanoparticles in dendrimers (usually PAMAM derivatives).²³ Now, we have tested one dendrimer containing only palladium(0) complexes on its surface and three batches of nanoparticles stabilized by dendrimers containing at

(20) Herein, we present an example of how the number of dendrimers per nanoparticle was calculated. For nanoparticles stabilized by the complexed dendrimer of the fourth generation, **6b-Gc₄**, the number of dendrimers per nanoparticle was calculated by dividing the number of atoms of Pd in the corresponding nanoparticles (nanoparticles of 3.2 nm diameter contain 1.1×10^3 atoms of Pd) by the number of palladium atoms in the molar formulation of the material/dendrimer (238, if the material was Pd₂₃₈(**6b-Gc₄**), data calculated from elemental analysis). In this case, we obtained a relation of 5 dendrimers/nanoparticle.

(21) (a) Maraval, V.; Laurent, R.; Caminade, A.-M.; Majoral, J.-P. *Organometallics* **2000**, *19*, 4025–4029. (b) Koprowsky, M.; Sebastián, R. M.; Maraval, V.; Zablocka, M.; Cadierno, V.; Donnadiou, B.; Igau, A.; Caminade, A.-M.; Majoral, J.-P. *Organometallics* **2002**, *21*, 4680–4687. (c) Laurent, R.; Caminade, A.-M.; Majoral, J.-P. *Tetrahedron Lett.* **2005**, *46*, 6503–6506. (d) Ouali, A.; Laurent, R.; Caminade, A.-M.; Majoral, J.-P.; Taillefer, M. *J. Am. Chem. Soc.* **2006**, *128*, 15990–15991.

(22) (a) Blanco, B.; Brissart, M.; Moreno-Mañas, M.; Pleixats, R.; Mehdi, A.; Reyé, C.; Bouquillon, S.; Hénin, F.; Muzart, J. *Appl. Catal., A* **2006**, *297*, 117–124. (b) Moreno-Mañas, M.; Pleixats, R.; Serra-Muns, A. *Synlett* **2006**, *18*, 3001–3004. (c) Masllorens, J.; González, I.; Roglans, A. *Eur. J. Org. Chem.* **2007**, 158–166.

Scheme 3. Heck Reaction Catalyzed by 6b-G₀ (Entry 3), Pd₇(6b-G₀)₁ (Entry 5), Pd₂₃₈(6b-Gc₄)₁ (Entry 16), and Pd₂(6a-G₀)₁/Pd₅(5a-G₀)₁ (Entry 2)^a



^a (a) Isolated yield of butyl cinnamate.

the same time palladium(0) complexes in their structures. The three first experiments were conducted in homogeneous media (all nanoparticles tested were completely soluble in THF), but the catalytic material obtained in entries 3, 5, and 16 (Table 1) was easily recovered and reused, and it could be precipitated using pentane. One last experiment was conducted in heterogeneous media using as the catalytic material Pd₂(6a-G₀)₁/Pd₅(5a-G₀)₁ of entry 2 (Scheme 3).

The Mizoroki–Heck reaction of iodobenzene with *n*-butyl acrylate in basic media (Bu₃N) was catalyzed by 2% of the palladium(0) atoms coming from the different materials presented just before. In all cases, the catalyst was recovered and reused five times without appreciable loss of activity. Conversions at 4 and 24 h and isolated yields of some of the runs performed are represented in Scheme 3 (see also the Supporting Information). Conversions were calculated by gas chromatography (GC) using undecane as the internal reference in all runs. The soluble catalysts (entries 3, 5, and 16) were more active than the heterogeneous one (entry 2). Nanoparticles stabilized by the complexed dendrimer of the zero generation 6b-G₀ (Pd₇(6b-G₀)₁, entry 5) gave better results than the discrete complexed dendrimer 6b-G₀ (entry 3). Working with NPs stabilized by a higher generation dendrimer, Pd₂₃₈(6b-Gc₄)₁ of entry 16, did not improve the final results. Moreover, conversion in the initial run was very low (10% after 4 h and 52% at 24 h) compared with that in the same run performed by using Pd₇(6b-G₀)₁ as the catalyst (34% after 4 h and 100% after 24 h); however, conversions improved in the following runs (Scheme 3). The small activity in the first run could be explained in this case by the presence of nanoparticles in the internal cavities of this dendrimer of the fourth generation,

less accessible, being more external and accessible in following runs. The migration of Au₅₅ nanoclusters from the internal cavities to the surface of phosphorus dendrimers of the same generation has been described by some of us.²⁴

Similar Heck reactions have been catalyzed by macrocycles complexed with palladium(0) (2, Figure 1); however, conversions were not always complete, and the catalyst could not be recycled. Decomplexation of palladium(0) was observed, and black palladium was formed. Free macrocycles were recovered by flash chromatography.¹¹

The last catalytic test was performed in heterogeneous media. Insoluble nanoparticles stabilized by a zero generation dendrimer (Pd₂(6a-G₀)₁, entry 2) were less active compared with materials of entries 5 and 16, and their activity seemed to be more or less constant after some runs; neither a clear increase nor a decrease was observed. (Scheme 3)

Catalytic tests performed, in a heterogeneous way, with Pd(0) NPs stabilized by model dendrimer 7-G₀ gave clearly the worst conversions (0% at 4 h and 58% at 24 h in the first cycle, 32% at 24 h in the fourth cycle); a total loss of activity was observed in the fifth run, and palladium black seemed to be formed. These results enhance the importance of the presence of our macrocycles on the surfaces of dendrimers, not only increasing in some cases the solubility of the nanoparticulated materials obtained and giving better quality nanoparticles, but also showing an important role in the stabilization of NPs run after run. Macrocycles could also play an important role in the reaction mechanism, probably by the stabilization of discrete palladium atoms that could take part in the catalytic cycle.

So, as a conclusion of this part of the work, under the same experimental conditions (0.21 M benzene iodide, 2% Pd(0) atoms as the catalyst), soluble nanoparticulated catalysts showed to be more active than heterogeneous ones. Under these conditions, soluble nanoparticles stabilized by the smaller dendrimer (6b-G₀, entry 5) resulted the more active material tested.

After recycling the catalysts five times, they were recovered mixed with a large amount of ammonium salts formed during the reactions. At that point, recovered dendrimer 6b-G₀ could not be analyzed due to the small amounts used in the first cycle (8 mg). However, its constant catalytic activity seemed to indicate that no big changes in its structure should have occurred. It could not be determined if it acted as a homogeneous catalyst or as a precatalyst. The other three recovered catalysts were analyzed by HR-TEM after the fifth run. No nanoparticles were observed from the recovered material of entry 5, probably due to the small quantity used in the first run (3 mg) and the presence of large amounts of tetraalkylammonium salts. However, from the analysis of the other two materials, we concluded that the recovered nanoparticles were clearly smaller than the starting ones. Before catalysis, the materials of entries 2 and 16 contained nanoparticles of 4.1 and 3.2 nm diameter, respectively; after the fifth run, the diameters were 2.3 and 2.4 nm, respectively (see the Supporting Information). The decrease in the size of the nanoparticles after catalytic cycles has been rarely observed.²⁵ This effect could explain, in the homogeneous catalysis tests, the increase in the speed of the reaction observed during the series of experiments, run after run. No information related to the stabilizing shell of these new nanoparticles is available at the moment. Nevertheless, ammonium salts obtained during the catalyzed reaction could also play any role.²⁶ The important role of dendrimers in the

(23) For a review on the use as catalysts of metal nanoparticles, specially entrapped nanoparticles in dendrimers: (a) Astruc, D.; Lu, F.; Ruiz Aranzaz, J. *Angew. Chem., Int. Ed.* **2005**, *44*, 7852–7872. (b) Scott, R. W. J.; Wilson, O. M.; Crooks, R. M. *J. Phys. Chem. B* **2005**, *109*, 692–704. (c) Lemo, J.; Heuze, K.; Astruc, D. *Inorg. Chim. Acta* **2006**, *359*, 4909–4911. (d) Wu, L.; Li, B. L.; Huang, Y. Y.; Zhou, H. F.; He, Y. M.; Fan, H. *Org. Lett.* **2006**, *8*, 3605–3608.

(24) Schmid, G.; Emmrich, E.; Majoral, J.-P.; Caminade, A.-M. *Small* **2005**, *1*, 73–75.

(25) (a) Narayanan, R.; El-Sayed, M. A. *J. Am. Chem. Soc.* **2003**, *125*, 8340–8347. (b) Thathagar, M. B.; Kooyman, P. J.; Boerleider, R.; Jansen, E.; Elsevier, C. J.; Rothenberg, G. *Adv. Synth. Catal.* **2005**, *347*, 1965–1968.

stabilization of these nanoparticles was probed when the same reaction was performed with Pd(OAc)₂ as the catalyst and tributylamine as the base in the presence of PPh₃ under inert atmosphere, and no formation of nanoparticles was observed after the reaction without the presence of dendrimers. In comparison with our catalytic tests, this reference experiment worked faster at the beginning of the reaction (82% conversion after 4 h) but the reaction stopped and only 92% conversion was observed after 24 h, probably due to the precipitation of palladium(0) black during the reaction. In this system, the catalyst could not be recovered.

The bad results obtained in the catalytic tests performed with Pd(OAc)₂ and NPs stabilized by **7-G₀** enhance the interest for the recoverable and reusable catalyst reported in this work.

3. Conclusions

New dendrimers containing up to 96 triolefinic 15-membered macrocycles on their surfaces have been prepared. These macromolecules have the ability to stabilize palladium(0) nanoparticles from 2.5 up to 7.9 nm in diameter. Dendrimers containing 2,4,6-triisopropylphenyl groups on their surfaces generated nanoparticulated materials soluble in common organic solvents; however, the presence of *p*-tolyl groups gave insoluble ones.

A new synthesis of palladium(0) nanoparticles stabilized by phosphorus dendrimers has been presented directly from palladium(0) sources, without the necessity of the addition of a reducing agent. Classical methods used are based on (i) the reduction of a high valence metal salt in the presence of the stabilizer; (ii) the hydrogenation of an unsaturated ligand in a metal(0) complex; or (iii) vapor metal deposition. Our method, here described, is based on the interchange of ligands in a discrete Pd(0) complex: Pd₂(dba)₄ or Pd(PPh₃)₄ and dendrimers containing macrocycles of type **1** on their surface. Indeed, macrocycles **1** are better ligands than dba, and therefore, transfer of the initial palladium atom to the macrocycle is favored. Triphenylphosphine is better as a ligand than macrocycles **1**. However, the transfer of metal to the macrocycle is favored by the oxidation of the phosphine to its oxide, a process difficult to avoid even by working under inert atmosphere. NPs formed from Pd₂(dba)₄ required generally shorter reaction times. The coordination of a first palladium atom by the macrocycles seems to favor the formation of small well-defined nanoparticles. The combination between the palladium(0) source and the stabilizer is important to obtain smaller and higher quality nanoparticles; however, no general rule could be proposed. NP size does not depend on the generation of dendrimers used as stabilizers. The methodology is highly reproducible.

These new materials have been used as easily recoverable homogeneous and heterogeneous catalysts in Mizoroki–Heck reactions; in general, the homogeneous ones are more active than the heterogeneous one as expected. Dendrimers containing only palladium(0) complexes on the surface, materials containing complexes and nanoparticles, or both are good catalysts; however,

the same dendrimer containing stabilized nanoparticles works faster. The use of nanoparticles stabilized by the fourth generation dendrimer as the catalyst did not improve conversions, so no dendritic effect is observed in this case. The diameter of the nanoparticles used as the catalyst decreased after several runs, an effect that could explain the increase of the activity of the nanoparticulated catalysts tested run after run. Further studies in catalysis will be reported in following works.

The presence of macrocycles in phosphorus dendrimers allows us to modulate the solubility of new nanoparticulated materials to favor the formation of good quality nanoparticles and their stabilization after catalytic cycles.

4. Experimental Section

General. Melting points were determined with a Kofler apparatus and are uncorrected. IR spectra were recorded in the attenuated total reflectance mode (ATR) in a Bruker Tensor 27 spectrometer. NMR spectra were recorded with a Bruker AC250 or Bruker AM400 instrument. ¹H NMR and ¹³C{¹H} NMR (62.5 MHz) chemical shifts are reported relative to tetramethylsilane; coupling constants are reported in Hz. ³¹P NMR spectra are reported relative to H₃PO₄ 85% in water. The attributions of ¹H NMR and ¹³C NMR spectra were done using distortionless enhancement by polarization transfer (DEPT), nuclear Overhauser effect (nOe), correlation spectroscopy (COSY), heteronuclear multiple quantum correlation (HMBC), heteronuclear multiple bond correlation (HMBC), and total correlation spectroscopy (TOCSY) experiments when necessary.

Matrix-assisted laser desorption ionization time-of-flight (MALDI-TOF) spectra were recorded on a BIFLEX spectrometer (Bruker-Franzen Analytik) equipped with a pulsed nitrogen laser (337 nm), operating in positive-ion reflector mode, using 19 kV acceleration voltage. Matrices (2,5-dihydroxybenzoic acid or ditranol) were prepared at 5 mg/mL in tetrahydrofuran (THF). Analytes were dissolved at concentrations between 0.1 and 5 mg/mL in THF or chloroform.

Elemental analyses for C, H, N, S, Pd, and P are the average of two determinations.

UV–vis spectra of **5b-G₀**, **6b-G₀** (entry 3), and **Pd₇(6b-G₀)₁** (entry 5) were obtained in 8453 Hewlett-Packard spectrometer in CH₂-ClCH₂Cl using 10⁻⁵ M concentrations.

TEM analyses were performed in the “Servei de Microscòpia” of the Universitat Autònoma de Barcelona using a Hitachi H-7000 model at 100 kV. Insoluble nanoparticulated materials were sonicated in THF for 2 min, and one drop of the finely divided suspension, or of the solution if the material was directly soluble in THF, was placed on a specially produced structureless carbon support film having a thickness of 4–6 nm and dried before observation.

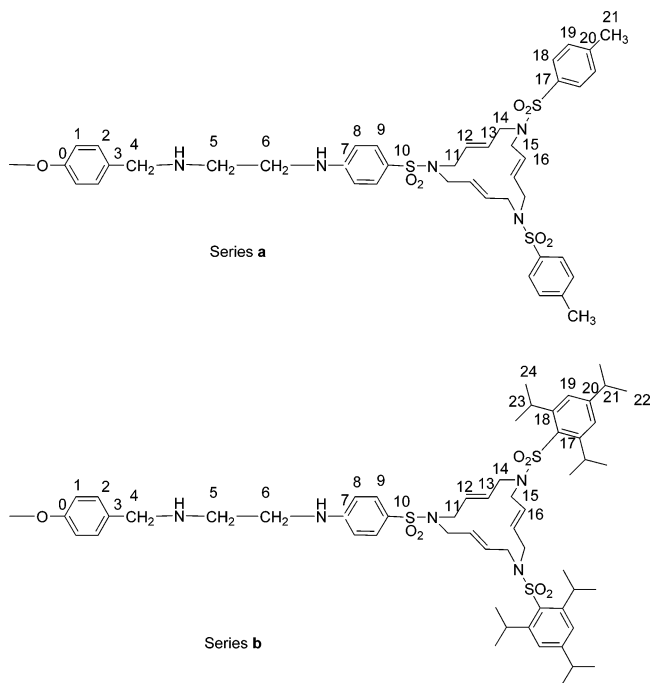
Yields of nanoparticles were determined as (palladium incorporated in nanoparticles/palladium introduced) × 100.

All preparations of dendrimers were performed under inert atmosphere. Complexes and nanoparticles were prepared with Schlenk type glassware. Anhydrous solvents were used thoroughly.

Compounds **3a**,¹¹ **3b**,¹³ **4-G₀**,¹⁴ **4-Gc₀**,¹⁵ **4-Gc₁**,¹⁶ and **4-Gc₄**¹⁶ were synthesized according to published procedures.

Preparation of 5a-G₀. (a) *Formation of the Imine Derivative.* Macrocycle **3a** (0.50 g, 0.70 mmol) in THF (10 mL) was added to a solution of **4-G₀** (0.10 g, 0.23 mmol) in THF (15 mL). The mixture was left overnight under stirring at room temperature. The solvent was evaporated to 1 mL, and then pentane was added until the formation of a white precipitate. The mixture was stirred for 10 min and filtered via cannula. The solid was washed twice with a mixture of THF–pentane (1:10) and dried to afford 0.39 g (66%) of the trisimine as a white solid that was not purified further. ¹H NMR (250 MHz, CDCl₃) δ 2.44 (s, 18H, H-21), 3.20–4.00 (m, 48H, H-5,6,11,14,15), 4.60–4.80 (NH), 5.40–5.70 (m, 18H, H-12,13,16), 6.50 (d, *J* = 7.5 Hz, 2H, H-8), 6.66 (d, *J* = 8.6 Hz, 4H, H-8), 7.20–7.43 (m, 8H, H1,2), 7.23 (d, *J* = 8.1 Hz, 12H, H-19), 7.55 (d, *J* = 8.6 Hz, 6H, H-9), 7.64 (d, *J* = 8.1 Hz, 12H, H-18), 7.70–7.82 (m, 4H,

(26) (a) Bönnemann, H.; Brijoux, R.; Brinkmann, R.; Dinjus, E.; Jousen, T.; Korall, B. *Angew. Chem., Int. Ed. Engl.* **1991**, *30*, 1312–1314. (b) Reetz, M. T.; Helbig, W. *J. Am. Chem. Soc.* **1994**, *116*, 7401–7402. (c) Reetz, M. T.; Helbig, W.; Quaiser, S. A.; Stimming, U.; Breuer, N.; Vogel, R. *Science* **1995**, *267*, 367–369. (d) Kiraly, Z.; Veisz, B.; Mastalir, Z.; Razga, Z.; Dékány, I. *Chem. Commun.* **1999**, 1925–1926. (e) Mukhopadhyay, S.; Rothenberg, G.; Gitis, D.; Sasson, D. *J. Org. Chem.* **2000**, *65*, 3107–3109. (f) Reetz, M. T.; Winter, M.; Breinbauer, R.; Thurn-Albrecht, T.; Vogel, W. *Chem.–Eur. J.* **2001**, *7*, 1084–1094. (g) Özkar, A.; Finke, R. G. *J. Am. Chem. Soc.* **2002**, *124*, 5796–5810. (h) Bras, J. L.; Mukherjee, D. K.; González, S.; Tristany, M.; Ganchev, B.; Moreno-Mañas, M.; Pleixats, R.; Hémin, F.; Muzart, J. *New J. Chem.* **2004**, *28*, 1550–1553. (i) Reetz, M. T.; De Vries, J. G. *Chem. Commun.* **2004**, 1559–1563.



H-1,2), 8.32 (br s, 3H, H-4). $^{31}\text{P}\{^1\text{H}\}$ NMR (101.3 MHz, CDCl_3) δ 52.8, 53.0 (possible *Z,E* isomers around $\text{C}=\text{N}$).

(b) *Reduction of the Imine Derivative.* The above trisimine (0.39 g, 0.15 mmol) in THF (10 mL) was added to NaBH_3CN (0.18 g, 2.80 mmol) in THF (5 mL). The mixture was magnetically stirred for 5 days at 70 °C and then cooled at room temperature. The solids were filtered off, and the filtrate was evaporated to 1 mL. Pentane was added, and a yellowish oil precipitated. The solvent was decanted off, and anhydrous ether (3 mL) was added. After 10 min of stirring, a white solid appeared. It was dissolved in acetone, leaving an insoluble residue that was filtered off. A mixture of ether–pentane (1:10) was added, and **5a-G₀** precipitated as a white solid (0.33 g, 84%). mp 115–118 °C. IR (ATR) 2848, 1595, 1330, 1153, 1088 cm^{-1} . ^1H NMR (250 MHz, $[\text{D}_8]\text{-THF}$) δ 2.51 (s, 18H, H-21), 2.96 (m, 6H, H-5), 3.37 (m, 6H, H-6), 3.71 (br s, 24H, H-11,14,15), 3.78 (br s, 12H, H-11,14,15), 3.91 (s, 6H, H-4), 5.50–5.75 (m, 18H, H-12,13,16), 5.90 (NH), 6.77 (d, $J = 8.8$ Hz, 6H, H-8), 7.31 (dd, $J_{\text{H-H}} = 8.3$ Hz, $J_{\text{H-P}} = 1.5$ Hz, 6H, H-1), 7.47 (d, $J = 8.2$ Hz, 12H, H-19), 7.51 (d, $J = 8.3$ Hz, 6H, H-2), 7.60 (d, $J = 8.8$ Hz, 6H, H-9), 8.78 (d, $J = 8.2$ Hz, 12H, H-18). $^{13}\text{C}\{^1\text{H}\}$ NMR (62.5 MHz, $[\text{D}_8]\text{-THF}$) δ 21.5 (C-21), 43.8 (C-6), 48.7 (C-5), 51.3 and 51.4 (C-11, 14, 15), 53.5 (C-4), 112.2 (C-8), 121.6 (d, $J_{\text{C-P}} = 4.8$ Hz, C-1), 125.9 (C-10), 128.1 (C-18), 129.9 (C-9), 130.1 (C-2), 130.4 (C-19), 130.6 and 130.9 (C-12,13,16), 138.0 (C-17), 140.0 (C-3), 144.0 (C-20), 150.5 (d, $J_{\text{C-P}} = 7.6$ Hz, C-0), 153.5 (C-7). $^{31}\text{P}\{^1\text{H}\}$ NMR (101.3 MHz, $[\text{D}_8]\text{-THF}$) δ 52.5. MALDI-TOF MS (matrix of dihydroxybenzoic acid): m/z calcd for $\text{C}_{123}\text{H}_{144}\text{N}_{15}\text{O}_{21}\text{PS}_{10}$, 2517.8 [M^+]; found, 2540.8 [$\text{M} + \text{Na}^+$].

Preparation of 5b-G₀. (a) *Formation of the Imine Derivative.* Macrocycle **3b** (0.39 g, 0.42 mmol) in THF (10 mL) was added to a solution of **4-G₀** (0.06 g, 0.14 mmol) in THF (10 mL). The mixture was stirred overnight. The solvent was evaporated to 1 mL, and pentane was added until the formation of a white precipitate. The mixture was stirred for 10 min and filtered via cannula. The solid was washed with THF–pentane (1:10) and dried to afford 0.39 g of the trisimine (89%) as a white solid. IR (ATR) 2954, 1598, 1313, 937 cm^{-1} . ^1H NMR (250 MHz, CDCl_3) δ 1.24 (d, $J = 6.7$ Hz, 36H, H-22), 1.26 (d, $J = 6.7$ Hz, 72H, H-24), 2.91 (sept, $J = 6.7$ Hz, 6H, H-21), 3.20–3.60 (m, 6H, H-5,6), 3.60–4.00 (m, 42H, H-5,6,11, 14,15), 4.11 (sept, $J = 6.7$ Hz, 12H, H-23), 4.70 (NH), 5.50–5.90 (m, 18H, H-12,13,16), 6.50 (d, $J = 8.2$ Hz, 2H, H-8), 6.65 (d, $J = 8.2$ Hz, 4H, H-8), 7.00–7.50 (m, 8H, H-1,2), 7.17 (s, 12H, H-19), 7.58 (d, $J = 8.2$ Hz, 6H, H-9), 7.77 (m, 4H, H-1,2), 8.32 (s, 3H, H-4). $^{31}\text{P}\{^1\text{H}\}$ NMR (101.3 MHz, CDCl_3) δ 52.9, 53.1 (possible *Z,E* isomers around $\text{C}=\text{N}$).

(b) *Reduction of the Imine Derivative.* The above trisimine (0.39 g, 0.12 mmol) in THF (10 mL) was added to a solution of NaBH_3CN (0.12 g, 1.91 mmol) in THF (5 mL). The mixture was stirred for 3 days at 70 °C. The solvent was evaporated, and the residue was washed with chloroform. The solution was decanted to eliminate solids and filtered through Celite, and the solvent was evaporated. The new residue was washed with THF–pentane (1:10) and dried to afford **5b-G₀** as a white solid (0.36 g, 91%). mp 124–126 °C. IR (ATR) 3381, 2959, 2866, 1596, 1305, 1149 cm^{-1} . ^1H NMR (250 MHz, CDCl_3) δ 1.23 (d, $J = 6.8$ Hz, 36H, H-22), 1.25 (d, $J = 6.8$ Hz, 72H, H-24), 2.80–3.00 (m, 12H, H-5,21), 3.15–3.30 (m, 6H, H-6), 3.60–3.90 (m, 42H, H-4,11,14,15), 4.08 (sept, $J = 6.7$ Hz, 12H, H-23), 4.81 (NH), 5.65–5.80 (m, 18H, H-12,13,16), 6.59 (d, $J = 8.8$ Hz, 6H, H-8), 7.15 (s, 12H, H-19), 7.19 (dd, $J_{\text{H-H}} = 8.5$ Hz, $J_{\text{H-P}} = 1.4$ Hz, 6H, H-1), 7.33 (d, $J = 8.5$ Hz, 6H, H-2), 7.54 (d, $J = 8.8$ Hz, 6H, H-9). $^{13}\text{C}\{^1\text{H}\}$ NMR (62.5 MHz, CDCl_3) δ 23.3 (C-22), 24.5 (C-24), 28.9 (C-23), 33.9 (C-21), 42.4 (C-6), 47.3 (C-5), 48.5 (C-14,15), 51.0 (C-11), 52.5 (C-4), 111.6 (C-8), 120.8 (d, $J_{\text{C-P}} = 4.8$ Hz, C-1), 123.4 (C-19), 125.2 (C-10), 128.7 (C-12, 13,16), 128.9 (C-9), 129.1 (C-2), 129.6 (C-12,13,16), 130.6 (C-17), 130.7 (12,13,16), 137.4 (d, $J_{\text{C-P}} = 1.9$ Hz, C-3), 149.4 (d, $J_{\text{C-P}} = 7.6$ Hz, C-0), 151.2 (C-18), 151.5 (C-7), 152.9 (C-20). $^{31}\text{P}\{^1\text{H}\}$ NMR (101.3 MHz, CDCl_3) δ 54.6. MALDI-TOF MS (matrix of dihydroxybenzoic acid): m/z calcd for $\text{C}_{171}\text{H}_{240}\text{N}_{15}\text{O}_{21}\text{PS}_{10}$, 3190.5 [M^+]; found, 3213.5 [$\text{M} + \text{Na}^+$], 3229.5 [$\text{M} + \text{K}^+$]. UV–vis ($\text{CH}_2\text{-ClCH}_2\text{Cl}$): λ_{max} (ϵ) = 224 (150 207), 237 (128 182), 276 nm (167 192 $\text{M}^{-1} \text{cm}^{-1}$).

Preparation of Complex 6b-G₀. A mixture of dendrimer **5b-G₀** (0.10 g, 3.13×10^{-2} mmol) and $\text{Pd}_2(\text{dba})_4$ (0.06 g, 0.11 mmol) in THF (3 mL) was stirred overnight at 60 °C. The crude reaction was filtered through Celite, and the solvent was evaporated to 1 mL. Pentane was then added, and the formed solid was filtered, washed with pentane, and dried to afford **6b-G₀** (0.05 g, 43%) as a brown solid. mp 189–192 °C. IR (ATR) 2958, 2866, 1596, 1458, 1305, 1151 cm^{-1} . ^1H NMR (250 MHz, CDCl_3) δ 1.10–1.35 (108H, H-22, 24), 1.60–1.75 (m, 3H, H-11,14,15), 2.00–2.20 (m, 9H, H-11, 14,15), 2.80–3.00 (m, 15H, H-5,21,12,13,16), 3.10–3.30 (m, 15H, H-6,11,12,13,14,15,16), 3.60–3.80 (m, 6H, H-12,13,16), 3.80–3.95 (m, 6H, H-4), 4.10–4.20 (m, 18H, H-12,13,16,23), 4.40–4.75 (m, 18H, H-11,14,15), 4.79 (NH), 6.55 (d, $J = 8.5$ Hz, 6H, H-8), 7.17 (s, 12H, H-19), 7.18 (d, $J = 8.5$ Hz, 6H, H-1), 7.32 (d, $J = 8.5$ Hz, 6H, H-2), 7.50 (d, $J = 8.5$ Hz, 4H, H-9), 7.56 (d, $J = 8.8$ Hz, 2H, H-9). $^{13}\text{C}\{^1\text{H}\}$ NMR (62.5 MHz, CDCl_3) δ 23.3 (C-24), 24.5 (C-22), 29.0 (C-23), 33.9 (C-21), 42.4 (C-6), 43.6 (C-11,14, 15), 45.0 (C-11,14,15), 46.3 (C-11,14,15), 47.2 (C-5), 47.5 (C-11, 14,15), 48.2 (C-11,14,15), 49.6 (C-11,14,15), 52.5 (C-4), 78.3 (C-16), 78.4–78.9 (m, C-13), 83.1 (C-12), 111.6 (C-8), 120.8 (d, $J_{\text{C-P}} = 3.8$ Hz, C-1), 123.7 (C-19), 128.8 (C-2), 129.1 (C-9), 130.8 (C-10), 131.0 (C-17), 137.4 (d, $J_{\text{C-P}} = 1.9$ Hz, C-3), 149.3 (d, $J_{\text{C-P}} = 7.6$ Hz, C-0), 151.0 (C-18), 151.5 (C-7), 152.9 (C-20). $^{31}\text{P}\{^1\text{H}\}$ NMR (101.3 MHz, CDCl_3) δ 54.7. MALDI-TOF MS (matrix of dihydroxybenzoic acid): m/z calcd for $\text{C}_{171}\text{H}_{240}\text{N}_{15}\text{O}_{21}\text{PS}_{10}\text{Pd}_2$, 3508.2 [M^+]; found, 3534.9 [$\text{M} + \text{Na}^+$] (badly defined). UV–vis ($\text{CH}_2\text{ClCH}_2\text{Cl}$): λ_{max} (ϵ) = 227 (107 566), 276 nm (87 167 $\text{M}^{-1} \text{cm}^{-1}$).

Preparation of 5a-Gc₀. (a) *Formation of the Imine Derivative.* Macrocycle **3a** (0.40 g, 5.4×10^{-1} mmol) in THF (2 mL) was added to cyclotriphosphazene **4-Gc₀** (0.08 g, 8.75×10^{-2} mmol) in the same solvent (1 mL). The mixture was stirred overnight at room temperature, the solvent was evaporated, and pentane was added until the formation of a white precipitate. The stirring was maintained for 10 more minutes, and the solid was filtered via cannula, washed twice with THF–pentane (1:10), and dried to afford 0.44 g (~100%) of the hexaimine. ^1H NMR (250 MHz, CDCl_3) δ 2.42 (s, 36H, H-21), 3.10–3.30 (m, 4H, H-5,6), 3.40–3.80 (m, 92H, H-5,6,11, 14,15), 5.03 (br s, NH), 5.55 (m, 36H, H-12,13,16), 6.40–6.70 (m, 12H, H-8), 6.70–7.80 (m, 36H, H-1,2,9), 7.31 (d, $J = 8.1$ Hz, 24H, H-19), 7.65 (d, $J = 8.1$ Hz, 24H, H-18), 8.19 (m, 6H, H-4). $^{31}\text{P}\{^1\text{H}\}$ NMR (101.3 MHz, CDCl_3) δ 9.52, 9.56, 9.63, 9.67 (possible *Z,E* isomers around $\text{C}=\text{N}$ bonds).

The hexaimine was used in the next step without further purification.

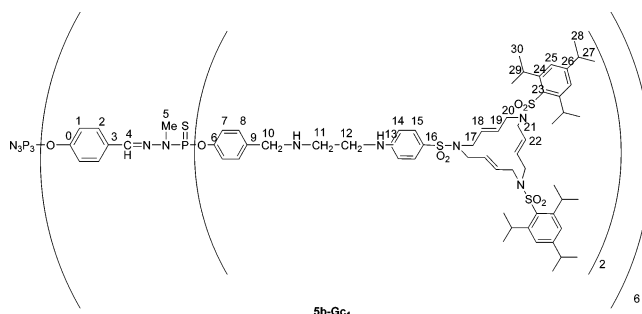
(b) *Reduction of the Imine Derivative.* The crude hexaimine (0.44 g, 8.75×10^{-2} mmol) in THF (8 mL) was added to a solution of NaBH_3CN (0.20 g, 3.18 mmol) in THF (2 mL). The mixture was stirred at 60 °C for 6 days. The solvent was evaporated, and the residue was washed twice with water for 5 min each and then with THF–pentane (1:10) to afford **5a-Gc₀** (0.29 g, 66%) as a white solid. mp 85–90 °C. IR (ATR) 3376, 2965, 1595, 1505, 1442, 1330, 1154, 1090 cm^{-1} . ^1H NMR (250 MHz, $[\text{D}_8]$ -THF) δ 2.46 (s, 36H, H-21), 2.89 (m, 12H, H-5), 3.30 (m, 12H, H-6), 3.55–3.85 (m, 84H, H-4, 11, 14, 15), 5.59 (m, 36H, H-12, 13, 16), 5.82 (NH), 6.72 (d, J = 8.7 Hz, 12H, H-8), 6.93 (d, J = 8.4 Hz, 12H, H-1), 7.26 (d, J = 8.4 Hz, 12H, H-2), 7.41 (d, J = 8.2 Hz, 24H, H-19), 7.56 (d, J = 8.7 Hz, 12H, H-9), 7.74 (d, J = 8.2 Hz, 24H, H-18). $^{13}\text{C}\{^1\text{H}\}$ NMR (62.5 MHz, $[\text{D}_8]$ -THF) δ 21.0 (C-21), 43.3 (C-6), 48.2 (C-5), 50.7 (C-14, 15), 50.8 (C-11), 53.1 (C-4), 111.7 (C-8), 121.0 (C-1), 125.4 (C-10), 127.5 (C-18), 129.3 (C-2), 129.4 (C-9), 129.5 (C-12, 13, 16), 129.8 (C-12, 13, 16), 130.0 (C-19), 130.4 (C-12, 13, 16), 137.4 (C-17), 138.0 (C-3), 143.5 (C-20), 149.9 (C-0), 152.9 (C-7). $^{31}\text{P}\{^1\text{H}\}$ NMR (101.3 MHz, $[\text{D}_8]$ -THF) δ 8.39. MALDI-TOF MS (matrix ditanol): m/z calcd for $\text{C}_{246}\text{H}_{288}\text{N}_{33}\text{O}_4\text{P}_3\text{S}_{18}$, 5044.5 $[\text{M}^+]$; found, 5067.6 $[\text{M} + \text{Na}^+]$.

Preparation of 5b-Gc₀. (a) *Formation of the Imine Derivative.* A solution of macrocycle **3b** (0.40 g, 0.43 mmol) in THF (3 mL) was added to a solution of cyclotriphosphazene **4-Gc₀** (0.06 g, 0.07 mmol) in THF (2 mL). The mixture was stirred overnight at room temperature. The solvent was evaporated to 1 mL, and pentane was added until the formation of a white precipitate. The mixture was stirred for an additional 10 min, and the solid was filtered via cannula, washed twice with THF–pentane (1:10), and dried to afford the hexaimine as a white solid (0.40 g, 93%). ^1H NMR (250 MHz, CDCl_3) δ 1.24 (apparent t, J = 6.0 Hz, 216H, H-22, 24), 2.84–3.01 (m, 18H, H-5, 21), 3.20–3.60 (m, 18H, H-5, 6), 3.60–4.00 (m, 72H, H-11, 14, 15), 4.12 (m, 24H, H-23), 4.70–5.00 (br s, NH), 5.75 (m, 36H, H-12, 13, 16), 6.44 (d, J = 9.2 Hz, 2H, H-8), 6.62 (br d, J = 8.7 Hz, 10H, H-8), 6.80–7.30 (m, 24H, H-1, 2), 7.20 (s, 24H, H-19), 7.54 (apparent t, J = 7.9 Hz, 12H, H-9), 8.19 (m, 6H, H-4). $^{31}\text{P}\{^1\text{H}\}$ NMR (101.3 MHz, CDCl_3) δ 9.48, 9.58, 9.62 (possible presence of isomers around C=N bonds).

(b) *Reduction of the Imine Derivative.* A solution of the above crude hexaimine (0.27 g, 0.05 mmol) in THF (10 mL) was added to a solution of NaBH_3CN (0.12 g, 1.83 mmol) in THF (2 mL). The mixture was stirred for 5 days at 60 °C. The solvent was evaporated, and the residue was digested with chloroform. The suspension was filtered through Celite, and the filtrate was evaporated. The residue was washed with THF–pentane (1:10) and dried to afford **5b-Gc₀** (0.13 g, 45%) as a white solid. mp 124–126 °C. IR (ATR) 3383, 2958, 1596, 1506, 1308, 1149 cm^{-1} . ^1H NMR (250 MHz, CDCl_3) δ 1.22 (d, J = 6.4 Hz, 72H, H-22), 1.24 (d, J = 6.4 Hz, 144H, H-24), 2.78–2.99 (m, 24H, H-5, 21), 3.18 (br s, 12H, H-6), 3.60–3.88 (m, 84H, H-4, 11, 14, 15), 4.08 (sept, J = 6.7 Hz, 24H, H-23), 4.89 (NH), 5.60–5.85 (m, 36H, H-12, 13, 16), 6.56 (d, J = 8.5 Hz, 12H, H-8), 6.91 (d, J = 8.2 Hz, 12H, H-1), 7.13 (d, J = 8.2 Hz, 12H, H-2), 7.15 (s, 24H, H-19), 7.52 (d, J = 8.5 Hz, 12H, H-9). $^{13}\text{C}\{^1\text{H}\}$ NMR (62.5 MHz, CDCl_3) δ 23.3 (C-22), 24.5 (C-24), 28.9 (C-23), 33.8 (C-21), 42.4 (C-6), 47.3 (C-5), 48.5 (C-14, 15), 51.0 (C-11), 52.5 (C-4), 111.6 (C-8), 120.7 (C-1), 123.7 (C-19), 125.0 (C-10), 128.7 (C-12, 13, 16), 128.8 (C-9), 128.9 (C-2), 129.5 (C-12, 13, 16), 130.5 (C-17), 130.7 (C-12, 13, 16), 136.4 (C-3), 149.4 (C-0, dd, $J_{\text{C-P}}$ = 4.8 Hz, $J_{\text{C-N}}$ = 2.8 Hz), 151.2 (C-18), 151.6 (C-7), 152.9 (C-20). $^{31}\text{P}\{^1\text{H}\}$ NMR (101.3 MHz, CDCl_3) δ 9.91. MALDI-TOF MS (matrix of dihydroxybenzoic acid): m/z calcd for $\text{C}_{342}\text{H}_{480}\text{N}_{33}\text{O}_4\text{P}_3\text{S}_{18}$, 6390.0 $[\text{M}^+]$; found, 6391.1 $[\text{M} + \text{H}^+]$, 6413.3 $[\text{M} + \text{Na}^+]$. MALDI-TOF MS (matrix of ditanol): m/z found, 6413.0 $[\text{M} + \text{Na}^+]$.

Preparation of 6b-Gc₀ (Entry 10). A mixture of **5b-Gc₀** (0.10 g, 1.56×10^{-2} mmol) and $\text{Pd}(\text{PPh}_3)_4$ (0.14 g, 1.25×10^{-1} mmol) in THF (7 mL) was refluxed under stirring for 2 days. The solution was filtered through Celite, and the solvent was evaporated to 1 mL. Pentane was added, and the formed precipitate was filtered and washed with pentane (some OPPh_3 remains) to afford 0.06 g (60%, calculated neglecting the OPPh_3) of **6b-Gc₀** as a brown solid. mp 180–195 °C. IR (ATR) 2958, 2865, 1596, 1505, 1429, 1309, 1151.

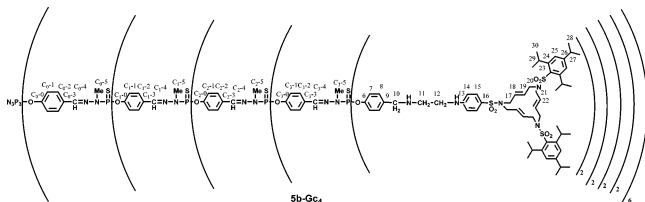
^1H NMR (250 MHz, CDCl_3) δ 1.10–1.40 (bs, 216H, H-22, 24), 1.60–1.75 (m, 6H, H-11, 14, 15), 2.00–2.20 (m, 18H, H-11, 14, 15), 2.75–3.00 (m, 30H, H-5, 12, 13, 16, 21), 3.05–3.40 (m, 30H, H-6, 11, 12, 13, 15, 16), 3.70–3.80 (m, 12H, H-12, 13, 16), 3.80–4.00 (m, 12H, H-4), 4.00–4.30 (m, 36H, H-23, H-12, 13, 16), 4.30–4.90 (m, 36H, NH and H-11, 14, 15), 6.50–7.90 (m, 72H, H-1, 2, 8, 9, 19 and POPh_3). $^{13}\text{C}\{^1\text{H}\}$ NMR (62.5 MHz, CDCl_3) δ 23.3 (C-24), 24.5 (C-22), 29.0 (C-23), 33.9 (C-21), 43.6–53.5 (C-4, 5, 6, 11, 14, 15), 78.3–83.1 (C-12, 13, 16), 111.6 (C-8), 120.8 (C-1), 123.7 (C-19), 128.8 (C-2), 129.1 (C-9), 130.8 (C-10), 131.0 (C-17), 137.4 (C-3), 149.3 (C-0), 151.0 (C-18), 151.5 (C-7), 152.9 (C-20). $^{31}\text{P}\{^1\text{H}\}$ NMR (101.3 MHz, CDCl_3) broad singlets at δ 8.96 (N_3P_3), 28.25 (POPh_3). MALDI-TOF MS could not be registered. Anal. Found: N, 5.34; S, 5.73; Pd, 12.4. Nanoparticles could not be detected by TEM.



Preparation of 5b-Gc₁. (a) *Formation of the Imine Derivative.* Macrocycle **3b** (0.10 g, 1.07×10^{-1} mmol) in THF (3 mL) was added to dendrimer **4-Gc₁** (0.03 g, 8.88×10^{-3} mmol) in THF (2 mL). The mixture was stirred overnight at room temperature. The solvent was evaporated, and the imine was used in the next step without further purification. ^1H NMR (250 MHz, CDCl_3) δ 1.10–1.40 (apparent t, J = 6 Hz, 432H, H-28, 30), 2.95 (m, 36H, H-11, 27), 3.34 (m, 24H, H-11, 12), 3.43 (m, 12H, H-11, 12), 3.60–3.90 (m, 162H, H-5, 17, 20, 21), 4.00–4.30 (m, 48H, H-29), 4.79 (br s, NH), 5.42 (m, 2H, H-18, 19, 22), 5.76 (m, 70H, H-18, 19, 22), 6.40 (d, J = 8.6 Hz, 6H, H-14), 6.60 (apparent t, J = 8.7 Hz, 18H, H-14), 6.85–7.30 (m, 108H, H-1, 7, 8, 25), 7.50–7.80 (m, 42H, H-2, 4, 15), 8.19 (br s, 12H, H-10). $^{31}\text{P}\{^1\text{H}\}$ NMR (101.3 MHz, CDCl_3) broad singlets at δ 9.67, 63.11, 63.40.

(b) *Reduction of the Imine Derivative.* The above crude dodecaimine (0.12 g, 8.83×10^{-3} mmol) in THF (10 mL) was added to NaBH_3CN (0.10 g, 1.60 mmol) in THF (2 mL). The mixture was stirred for 5 days at 60 °C. The solvent was evaporated, and the residue was digested with anhydrous chloroform. Salts were eliminated by passing through Celite, and the filtered solution was evaporated. The residue was washed with THF–pentane (1:10) and dried to afford **5b-Gc₁** (0.09 g, 73%) as a white solid. mp 128–130 °C. IR (ATR) 3383, 2959, 1597, 1504, 1460, 1420, 1304, 1191, 1149 cm^{-1} . ^1H NMR (250 MHz, CDCl_3) δ 1.23 (apparent t, J = 6.2 Hz, 432H, H-28, 30), 2.80–3.00 (m, 48H, H-11, 27), 3.10–3.30 (m, 42H, H-5, 12), 3.60–3.85 (m, 168H, H-10, 17, 20, 21), 3.95–4.20 (m, 48H, H-29), 4.94 (br s, NH), 5.60–5.85 (m, 72H, H-18, 19, 22), 6.55 (d, J = 8.2 Hz, 24H, H-14), 6.91 (d, J = 8.1 Hz, 12H, H-2), 7.09 (d, J = 8.1 Hz, 24H, H-7), 7.14 (s, 48H, H-25), 7.23 (d, J = 8.1 Hz, 24H, H-8), 7.52 (d, J = 8.1 Hz, 24H, H-15), 7.55–7.70 (m, 18H, H-1, 4). $^{13}\text{C}\{^1\text{H}\}$ NMR (62.5 MHz, CDCl_3) δ 23.3 (C-28), 24.5 (C-30), 29.0 (C-29), 32.7 (C-5), 33.9 (C-27), 41.9 (C-12), 47.0 (C-11), 48.5 (C-20, 21), 51.1 (C-17), 52.3 (C-10), 111.7 (C-14), 121.0 (C-1), 121.1 (C-7), 123.7 (C-25), 124.7 (C-16), 128.0 (C-2), 128.7 (C-18, 19, 22), 128.8 (C-15), 129.3 (C-8), 129.5 (C-18, 19, 22), 130.5 (C-23), 130.7 (C-18, 19, 22), 132.0 (C-3), 137.4 (C-9), 138.8 (C-4), 149.6 (C-6), 150.9 (C-0), 151.2 (C-24), 151.5 (C-13), 152.9 (C-26). $^{31}\text{P}\{^1\text{H}\}$ NMR (101.3 MHz, CDCl_3) δ 9.89, 63.71. MALDI-TOF MS (matrix ditanol): m/z calcd for $\text{C}_{732}\text{H}_{1008}\text{N}_{75}\text{O}_9\text{P}_9\text{S}_{42}$, 13 911.2 $[\text{M}^+]$; found, 13 935.0 (broad) $[\text{M} + \text{Na}^+]$, 13 953.2 $[\text{M} + \text{K}^+]$.

Preparation of 5b-Gc₄. (a) *Formation of the Imine Derivative.* Macrocycle **3b** (0.20 g, 2.13×10^{-1} mmol) and dendrimer **4-Gc₄** (0.055 g, 1.78×10^{-3} mmol) were dissolved in THF (0.5 mL). The



mixture was stirred at room temperature for 5 days. The solvent was concentrated to 0.25 mL, and pentane was added until the formation of a white precipitate. The mixture was stirred for an additional 10 min, and the solid was filtered via cannula, washed twice with THF-pentane (1:10), and dried to afford the dendrimer containing 96 imines on the surface as a white solid 0.20 g (94%). ^1H NMR (250 MHz, CDCl_3) δ 1.25 (t, $J = 6.5$ Hz, 3456H, H-28,30), 2.70–3.10 (m, 384H, H-11,27), 3.10–3.50 (m, 462H, H-12, H_{0-3-5}), 3.70–3.90 (m, 1152H, H-17,20,21), 3.90–4.20 (m, 384H, H-29), 4.80 (bs, NH), 5.60–5.80 (m, 576H, H-18,19,22), 6.30–7.90 (1602H, aromatic and H_{0-3-4}), 8.20 (s, 96H, H-10, $\text{CH}=\text{N}$). $^{31}\text{P}\{^1\text{H}\}$ NMR (81 MHz, CDCl_3) δ (bs) 64.95, 65.79 (possible presence of isomers around $\text{C}=\text{N}$ bonds). N_3P_3 was not observed.

(b) Reduction of the Imine Derivative. To a solution of the above dendrimer containing imines (0.20 g, 1.67×10^{-3} mmol) in CH_2Cl_2 (1 mL) was added a solution of 1 M Me_2SBH_3 in CH_2Cl_2 (100 μL , 0.01 mol). The mixture was stirred for 5 days at room temperature. An amount of 2 mL of MeOH was then added to the solution, and the mixture was stirred during 10 min. The solvent was evaporated, and this last process was repeated twice more. Compound **5b-Gc₄** (0.15 g, 75%) was isolated as a white solid. mp 142–143 °C. IR (ATR) 3380, 2957, 2867, 1598, 1503, 1461, 1310, 1147 cm^{-1} . ^1H NMR (500 MHz, CDCl_3) δ 1.15–1.31 (m, 3456H, H-28,30), 2.80–2.98 (m, 192H, H-27), 3.00–3.10 (m, 192H, H-11), 3.15–3.35 (m, 462H, H_{0-3-5} , H-12), 3.60–3.90 (m, 1344H, H-10,17,20,21), 4.00–4.20 (sept, $J = 6.4$ Hz, 384H, H-29), 4.80–5.20 (NH), 5.74 (bs, 576H, H-18,19,22), 6.50–7.90 (m, 1602H, aromatic and H_{0-3-4}). $^{13}\text{C}\{^1\text{H}\}$ NMR (125 MHz, CDCl_3) δ 23.5 (C-28), 24.8 (C-30), 29.2 (C-29), 30.0 (C_{0-3-5}), 34.1 (C-27), 40.7 (C-11), 45.1 (C-12), 48.8 (C-20,21), 51.2 (C-10,17), 112.0 (C-14), 121.0–122.0 (C_{0-3-1} , C-7), 123.9 (C-25), 125.5 (C-16), 127.5–128.0 (C_{0-3-2}), 129.0 (C-18,19,22), 129.2 (C-15), 129.3 (C-8), 129.8 (C-18,19,22), 130.4 (C-23), 130.9 (C-18,19,22), 132.4 (C_{0-3-3}), 139.0 (C_{0-3-4} , C-9), 150.0–150.6 (C_{0-3-0} , C-6), 151.7 (C-24), 151.8 (C-13), 153.2 (C-26). $^{31}\text{P}\{^1\text{H}\}$ NMR (101.3 MHz, CDCl_3) δ 65.93. N_3P_3 was not observed. $\text{C}_{6192}\text{H}_{8400}\text{N}_{663}\text{O}_{762}\text{P}_{93}\text{S}_{379}$ could not be identified by MALDI-TOF MS (matrix ditanol).

Preparation of 6b-Gc₄ (Entry 15). A mixture of **5b-Gc₄** (0.03 g, 2.50×10^{-7} mmol) and $\text{Pd}_2(\text{dba})_4$ (0.17 g, 2.89×10^{-5} mmol) in THF (3 mL) was refluxed under stirring for 1 night. The solution was filtered through Celite, and the solvent was evaporated to 1 mL. Pentane was added, and the formed precipitate was filtered and washed with pentane to afford 0.03 g of **6b-Gc₄** (92%) as a brown solid. mp 165–170 °C (decomposition). IR (ATR) 2957, 2868, 1598, 1503, 1460, 1314, 1191, 1149, 907 cm^{-1} . ^1H NMR (500 MHz, CDCl_3) δ 1.26 (t, $J = 6.5$ Hz, 3456 H, H-28,30), 1.60–1.80 (m, 96H, H-17,20,21), 1.90–2.25 (m, 288H, H-17,20,21), 2.75–3.00 (m, 480H, H-11,17,20,21,27), 3.05–3.35 (m, 750H, H_{0-3-5} , H-12, H-17,20,21, H-18,19,22), 3.70–3.95 (m, 384H, H-10,18,19,22), 4.00–4.30 (m, 576H, H-18,19,22,29), 4.35–4.90 (m, 576H, H-17,20,21, NH), 6.50–7.90 (1602H, aromatic and H_{0-3-4}). $^{13}\text{C}\{^1\text{H}\}$ NMR (125 MHz, CDCl_3) δ 24.0 (C-30), 25.3 (C-28), 29.2 (C-29), 33.5 (C_{0-3-5}), 34.6 (C-27), 43.8 (C-12), 44.4 (C-17,20,21), 45.7 (C-17,20,21), 46.1 (C-17,20,21), 47.0 (C-11), 48.4 (C-17,20,21), 49.0 (C-17,20,21), 50.4 (C-10), 78.7–80.0 (m, C-19,22), 83.8 (C-18), 112.4 (C-14), 121.0–123.0 (m, C_{0-3-1} , C-7), 124.4 (C-25), 128.0–130.5 (m, C_{0-3-2} , C-8,15), 131.0–132.0 (C_{0-3-3} , C-16,23), 139.5 (C_{0-3-4} , C-9), 149.0–151.0 (C_{0-3-0} , C-6), 151.6 (C-24), 151.7 (C-13), 153.7 (C-26). $^{31}\text{P}\{^1\text{H}\}$ NMR (81 MHz, CDCl_3) δ 60.4. N_3P_3 was not observed. A small quantity of palladium(0) nanoparticles was detected by TEM (5.8 ± 0.7 nm, THF, average calculated for 26 particles).

Nanoparticles of Entry 1. *General Method.* A mixture of **5a-G₀** (0.10 g, 0.04 mmol) and $\text{Pd}_2(\text{dba})_4$ (0.08 g, 0.14 mmol) in THF (4 mL) was stirred overnight at 60 °C. The liquid was decanted off, and the precipitated solid was washed with THF to afford 0.05 g (35%) of nanoparticles. Dec range 248–250 °C. IR (ATR) 2915, 1594, 1330, 1154, 1090 cm^{-1} . Elemental analysis found: P, 0.68; Pd, 10.97. TEM: 4.2 ± 0.7 nm (THF, average calculated for 117 particles). See Figure 2. MALDI-TOF spectroscopy of the small quantity of the residue obtained from the evaporation of the decanted liquid permitted identification of the presence of **6a-G₀**. MALDI-TOF MS (matrix of dihydroxybenzoic acid): m/z calcd for $\text{C}_{123}\text{H}_{144}\text{N}_{15}\text{O}_2\text{PPd}_3\text{S}_{10}$, 2835.5 [M^+], 2729.6 [$\text{M} - \text{Pd}^+$], 2623.7 [$\text{M} - 2\text{Pd}^+$], 2517.8 [$\text{M} - 3\text{Pd}$]; found, (broad signals) 2863.5 [$\text{M} + \text{Na}^+$], 2757.1 [$\text{M} - \text{Pd} + \text{Na}^+$], 2649.9 [$\text{M} - 2\text{Pd} + \text{Na}^+$], 2543.8 [$\text{M} - 3\text{Pd} + \text{Na}^+$], 2511.7 [$\text{M}^+ - 3\text{Pd}$]. See Figure 2a and b.

Nanoparticles of Entry 2. A yield of 0.07 g (59%) was obtained. Dec range >300 °C. IR (ATR) 2915, 1594, 1330, 1154, 1090 cm^{-1} . Elemental analysis found: P, 0.66%; Pd, 11.37%. TEM: 4.1 ± 0.7 nm (THF, average calculated for 175 particles). See Figure 2c and d.

Nanoparticles of Entry 4. *General Method.* A mixture of **5b-G₀** (0.05 g, 0.016 mmol) and $\text{Pd}_2(\text{dba})_4$ (0.09 g, 0.16 mmol) in THF (6 mL) was stirred overnight at 60 °C. The liquid was filtered through Celite, the filtrate was evaporated to 1 mL, and then pentane was added until precipitation. The solid was filtered and washed with pentane to afford 0.03 g (36%). Dec range 190–198 °C. IR (ATR) 2958, 2866, 1596, 1458, 1308, 1151 cm^{-1} . ^1H NMR data are the same as those for **6b-G₀**. Elemental analysis found: P, 0.57; Pd, 19.35. TEM: 4.3 ± 0.7 nm (THF, average calculated for 629 particles). See Figure 3a and b.

Nanoparticles of Entry 5. A yield of 0.18 g (98%) was obtained. Dec range 190–200 °C. IR (ATR) 2955, 2867, 1597, 1460, 1310, 1148 cm^{-1} . ^1H NMR data are the same as those for **6b-G₀** (a small amount of dba was retained on the solid). UV-vis ($\text{CH}_2\text{ClCH}_2\text{Cl}$): λ_{max} (ϵ) = 228 (136 718), 272 nm (87 494 $\text{M}^{-1} \text{cm}^{-1}$) (side band). Elemental analysis found: P, 0.84; Pd, 29.32. TEM: 3.4 ± 0.6 nm (THF, average calculated for 236 particles). See Figure 3c.

Nanoparticles of Entry 7. A yield of 0.05 g (62%) was obtained. Dec range 190–200 °C. IR (ATR) 2958, 2864, 1594, 1429, 1307, 1151 cm^{-1} . ^1H NMR data are the same as those for **5b-G₀**; broader signals were obtained. Elemental analysis found: N, 3.52; S, 5.07; Pd, 22.00. TEM: 2.5 ± 0.4 nm (THF, average calculated for 265 particles). See Figure 3d.

Nanoparticles of Entry 8. A yield of 0.10 g (77%) was obtained. Dec range >310 °C. IR (ATR) 2958, 2865, 1596, 1505, 1429, 1309, 1151 cm^{-1} . Elemental analysis found: P, 1.00; Pd, 15.83. TEM: 3.9 ± 1.0 nm (THF, average calculated for 132 particles).

Nanoparticles of Entry 9. A yield of 0.07 g (98%) was obtained. Dec range 240–250 °C. IR (ATR) 2958, 2867, 1597, 1310, 1154 cm^{-1} . ^1H NMR data are the same as those for **6b-Gc₀**. Elemental analysis found: P, 0.82; Pd, 16.17. TEM: 5.7 ± 0.6 nm (THF, average calculated for 629 particles). See Figure 4a.

Nanoparticles of Entry 12. A yield of 0.10 g (97%) was obtained. Dec range 180–190 °C. IR (ATR) 2958, 2865, 1596, 1505, 1429, 1309, 1151 cm^{-1} . ^1H NMR data are the same as those for **6b-Gc₀**. Elemental analysis found: N, 3.74; S, 4.63; Pd, 25.39. TEM: 2.9 ± 0.5 nm (THF, average calculated for 271 particles). See Figure 4b–d.

Nanoparticles of Entry 13. A yield of 0.04 g (40%) was obtained. Dec range 210–220 °C. IR (ATR) 2956, 2868, 1598, 1503, 1461, 1315, 1149 cm^{-1} . ^1H NMR (250 MHz, CDCl_3) δ 1.27 (bs, 432H, H-28,30), 1.60–1.75 (m, 12H, CH_2 in the cycle), 1.95–2.20 (m, 36H, CH_2 in the cycle), 2.75–3.00 (m, 60H, H-11,27, CH in the cycle), 3.10–3.30 (m, 72H, H-5,12, CH and CH_2 in the cycle), 3.65–3.70 (m, 24H, CH in the cycle), 3.80–3.93 (m, 24H, H-10), 4.10–4.30 (m, 72H, H-29, CH in the cycle), 4.35–4.90 (m, 72H, CH_2 in the cycle, NH), 6.40–7.70 (m, 174H, H-1,2,4,7,8,14,15,25). Elemental analysis found: P, 1.64; Pd, 10.66. TEM: 3.4 ± 0.4 nm (THF, average calculated for 155 particles). See Figure 5a.

Nanoparticles of Entry 14. A yield of 0.07 g (92%) was obtained. Dec range 220–230 °C. IR (ATR) 2958, 2866, 1596, 1503, 1430,

1308, 1151 cm^{-1} . ^1H NMR (250 MHz, CDCl_3) δ 1.10–1.40 (bs, 432H, H-28,30), 1.80–2.20 (m, 48H, CH_2 in the cycle), 2.75–3.00 (m, 60H, H-11,27 and CH in the cycle), 3.05–3.40 (m, 60H, H-5,12, CH and CH_2 in the cycle), 3.80–4.80 (m, 210H, NH, H-10,29, CH and CH_2 in the cycle), 6.50–7.80 (m, 174H, H-1,2,4,7,8,14,15,25 and POPh_3). Elemental analysis found: N, 4.61; S, 5.17; Pd, 14.80. TEM: 7.9 ± 2.2 nm (THF, average calculated for 62 particles). See Figure 5b.

Nanoparticles of Entry 16. A mixture of **6b-Gc₄** (0.015 g, 1.16×10^{-4} mmol) and $\text{Pd}_2(\text{dba})_4$ (0.19 g, 3.33×10^{-1} mmol) in THF (1.5 mL) was stirred overnight at 60 °C. The solution was filtered through Celite, the filtrate was evaporated to 1 mL, and then pentane was added until precipitation. The solid was filtered and washed with pentane to afford 0.03 g (89%). Dec point >300 °C. IR (ATR) 2957, 2868, 1598, 1503, 1460, 1314, 1191, 1149, 907 cm^{-1} . ^1H NMR data are the same as those for **6b-Gc₄**. Elemental analysis found: P, 1.29; Pd, 15.90. TEM: 3.2 ± 0.5 nm (THF, average calculated for 177 nanoparticles). See Figure 5c and d.

Preparation of *n*-Butyl Cinnamate under Catalysis by Pd_{238} -(6b-Gc₄**)₁ of Entry 16 and Recovery of the Catalytic Material (Run 2).** A mixture of iodobenzene (0.09 g, 0.5 mmol), butyl acrylate (0.08 g, 0.6 mmol), tributylamine (0.1 g, 0.5 mmol), Pd_{238} (**6b-Gc₄**)₁ of entry 14 (0.006 g, 0.009 mmol of Pd, 2 mol %), and THF (2 mL) was heated at reflux for 24 h. The evolution of the reaction conversion was followed by GC, using undecane as the internal reference (0.07 g, 0.5 mmol). After cooling, pentane (5 mL) was added, and then the catalyst and inorganic salts were filtered and washed twice with pentane (5 mL); this solid was used as the catalyst in the next run. The organic solutions were evaporated, and the residue was purified by column chromatography on silica gel with hexane–ethyl acetate

(95:5) as the eluent to afford *n*-butyl cinnamate (82% yield) as a colorless oil. IR (ATR) 2966, 2867, 1710, 1637, 1172 cm^{-1} . ^1H NMR (250 MHz, CDCl_3) δ 0.97 (t, $J = 7.4$ Hz, 3H), 1.44 (m, 2H), 1.70 (m, 2H), 4.21 (t, $J = 6.6$ Hz, 2H), 6.44 (d, $J = 16.0$ Hz, 1H), 7.38 (m, 3H), 7.53 (m, 2H), 7.69 (d, $J = 16.0$ Hz, 1H).

Acknowledgment. Financial support from the Ministry of Science and Technology (then Ministry of Education and Science) of Spain (Projects 2002BQU-04002, CTQ-2005-04968/BQU, HF2004-0212, and Consolider INGENIO 2010: CSD2007-00006) and *Generalitat de Catalunya* (Projects 2001SGR00181 and 2005SGR00305) is acknowledged. One of us (R.M.S.) was incorporated to the research group through a “Ramon y Cajal” contract (MCyT-FEDER/FSE). The Ministry of Education and Science of Spain is also gratefully acknowledged for predoctoral scholarships to E.B.

Supporting Information Available: NMR, IR, and MALDI-TOF spectra of compounds **5a,b-G₀**, **6b-G₀**, **5a,b-Gc₀**, **6b-Gc₀**, **5b-Gc₁**, **5b-Gc₄**, and **6b-Gc₄**; experimental description of the synthesis of compound **7-G₀** and its intermediates (NMR, IR spectra, and MALDI-TOF); UV–vis spectra of **5b-G₀**, **6b-G₀**, and Pd_7 (**6b-G₀**); some NMR and IR spectra of nanoparticulated materials; HR-TEM and electron diffraction images of entries 1, 2, 4, 5, 7–9, and 12–16 of Table 1, nanoparticles obtained from **7-G₀**, and the recovered materials isolated after catalytic tests from materials of entries 2 and 16; and tables containing complete results of catalytic tests. This material is available free of charge via the Internet at <http://pubs.acs.org>.

LA7013418